CHALMERS
UNIVERSITY OF TECHNOLOGY

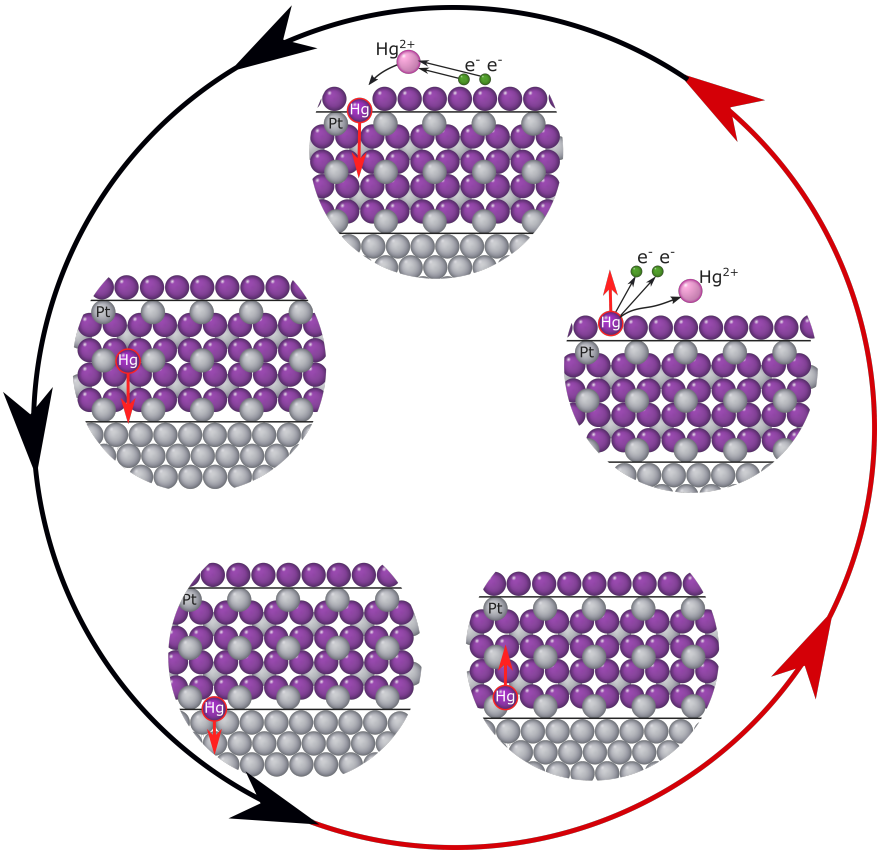

Regeneration of Foam Electrodes Used for for the Removal of Mercury from Aqueous Solutions

A study of the regenerative capacity of Platinum plated foam electrodes in mercury waste removal via electrochemical alloy formation.

Master's thesis in Physics

Pontus Gustafsson

DEPARTMENT OF PHYSICS
CHALMERS UNIVERSITY OF TECHNOLOGY
Gothenburg, Sweden 2024
www.chalmers.se

Master's thesis 2024

Regeneration of Foam Electrodes Used for for the Removal of Mercury from Aqueous Solutions

A study of the regenerative capacity of Platinum plated foam electrodes in mercury waste removal via electrochemical alloy formation.

PONTUS GUSTAFSSON

CHALMERS
UNIVERSITY OF TECHNOLOGY

Department of Physics
Division of Chemical Physics
Chalmers University of Technology
Gothenburg, Sweden 2024

Regeneration of Foam Electrodes Used for for the Removal of Mercury from Aqueous Solutions
A study of the regenerative capacity of Platinum plated foam electrodes in mercury waste removal via electrochemical alloy formation.
PONTUS GUSTAFSSON

Supervisor: Vera Roth, Department of Physics
Examiner: Björn Wickman, Department of Physics

Master's Thesis 2024
Department of Physics
Division of Chemical Physics
Chalmers University of Technology
SE-412 96 Gothenburg
Telephone +46 31 772 1000
Cover: Representation of the formation/regeneration mechanism on an atomic level. The three steps marked with a black arrow are formation and the two marked in red regeneration.

Typeset in LaTeX
Gothenburg, Sweden 2024

Regeneration of Foam Electrodes Used for for the Removal of Mercury from Aqueous Solutions
A study of the regenerative capacity of Platinum plated foam electrodes in mercury waste removal via electrochemical alloy formation.
PONTUS GUSTAFSSON
Department of Physics
Chalmers University of Technology

Abstract

Mercury is a heavy metal of great environmental concern. It possesses great environmental mobility and is highly toxic for both humans and wildlife. An electrochemical mercury decontamination technique that uses Pt-Hg alloy formation to collect mercury from aqueous sources has been developed and shows great promise and many advantages over existing techniques. The goal of this thesis is to study the regenerative capacity of platinum-coated foam electrodes used in this technique over decontamination cycles. Regeneration in this case refers to the re-release of mercury in the form of Hg-ions via the oxidation of Pt-Hg alloy. Using a three-electrode set-up in batch experiments, mercury was removed from 0.5 M sulphuric acid with a mercury concentration of 1000 ppb using a platinum-coated stainless steel foam. Mercury was also removed from contaminated concentrated sulphuric acid from a zinc smelter using a platinum-coated RVC foam. Unfortunately, complete regeneration was not achieved in any experiment, typically releasing less than half of the collected mercury. This partial regeneration is likely due to suboptimal experimental conditions. Despite this, the stability of the foams was demonstrated over multiple formations/regenerations. The problems identified also highlight possible ways forward for future research on the studied mercury decontamination technique. Decontamination with the RVC foam in concentrated sulphuric acid managed to reach mercury levels below the industry standard for high purity, something that has not been presented in previously published research.

Keywords: mercury, heavy metal, electrochemistry, decontamination, water treatment, regeneration.

Acknowledgements

First and foremost I want to thank my examiner Björn Wickman and supervisor Vera Roth for their sympathy and understanding when health and life have come in the way of the project. Without this understanding when I needed a break, and unquestioned enthusiastic welcome back when I was ready, this thesis would have never been finished. I am forever grateful. I also want to thank Björn for going above and beyond in his support and involvement in the finishing stages of the thesis. Similarly, I want to extend a further thank you to Vera for carrying out all the ICPMS analyses during the laboratory part of the project. The many hours in the lab on my behalf have not gone unnoticed, and you have my sincere thank you. I want to thank Julia Järlebark for bringing me into the project in the first place during my bachelor thesis and for agreeing to participate as an opponent for my presentation, without any personal gain. I also want to thank the team at Atium for their involvement in the project and especially Henric Ernbrink for providing laboratory supplies and equipment. Lastly, I want to thank my family and friends for always believing in me and pushing me to get this thesis finished, even when I started to doubt that it would ever happen.

Pontus Gustafsson, Gothenburg, August 2024

Contents

List of Figures

List of Acronyms

Below is the list of acronyms that have been used throughout this thesis listed in alphabetical order:

CE	Counter electrode
ICP-MS	Inductivly coupled plasma mass spectrometry
LSV	Linear sweep voltammetry
PVD	Physical vapour deposition
RE	Reference electrode
SHE	Standard hydrogen electrode
SS	Stainless steel
WE	Working electrode

1
Introduction

This master thesis project concerns itself with the highly relevant problem of mercury decontamination. Mercury is a toxic heavy metal with high mobility that bio-accumulates in the food chain of marine life and is considered one of the top ten chemicals of major public health concern by the World Health Organisation [1]. To mediate this problem, new and more effective decontamination methods for selective and effective removal of mercury from aqueous streams are needed. This project explores and searches to gain further knowledge about, one such method developed by Christian Tunsu and Björn Wickman in 2018 [2]. The method utilises electrochemical alloy formation to bind mercury to a platinum electrode. The bound mercury can then be released into a small amount, easily manageable, solution while the regenerated platinum electrode can be reused. Multiple studies have been done on the alloy formation, and the technique's decontamination ability in different conditions, but no study has yet focused on the regeneration of the platinum electrode. This thesis stands to begin to fill that gap in knowledge concerning the regenerative capabilities of the method.

1.1 Scope and Aim

The aim is to gain a broader understanding of the regeneration process for the Pt-Hg system. One of the main questions explored is; What happens to the Platinum electrode's decontamination capacity after multiple regenerations? To do this, multiple formations and regenerations were carried out on the same electrode, tracking its performance over multiple cycles.

1.1.1 Limitations

The formation of the alloy was not studied in detail, since much of the prior research has already focused on this aspect of the process. The main focus is to study the regeneration process on Pt-coated Reticulated Vitreous Carbon (RVC) foams and stainless steel foams. While other foams might be of interest it is beyond the scope of this thesis work.

1.1.2 Outline

This section functions as a road map for the rest of this report. In the next chapter, Background, the necessary foreknowledge about mercury and the environmental

problems it constitutes is provided. Information about mercury and its effect on the environment and people is also included here. This is followed by an overview of the main other available techniques for mercury decontamination to be able to compare and evaluate the presently studied technique. A brief comparison of this kind concludes the chapter. The theory chapter provides necessary electrochemical theory. The measurement techniques that have been employed and relevant theories concerning these are also a major part of this chapter. The theory chapter also includes a summary of previous research into this electrochemical mercury decontamination technique. The methods chapter then describe how these instruments and techniques have been employed for the measurements that make out the experimental part of this thesis. Some practical choices are also motivated and explained. The results and discussion chapter, contain the results of the decontamination and regeneration experiments together with interpretations of said results. The focus is on the regeneration part of the process since the study of this step is novel to this thesis. Finally, the conclusion and outlook chapter summarises the findings and provides suggestions on further work to be done in an outlook.

2
Background

This chapter aims to provide a suitable background into the problems connected to mercury. The chapter is initiated with a short history of mercury and the element's properties. This is followed by information about the environmental cycling of mercury and an overview of the largest sources of mercury pollution. The problems mercury pollution cause is highlighted by looking at mercury both from an environmental and from a human health perspective. A summary of some other decontamination techniques currently in use is also part of this chapter before the technique studied is presented. First, the working principle is explained before the chapter is concluded with a comparison to the other techniques previously mentioned.

2.1 Mercury

This section focuses on the element of interest, Mercury. The section begins with a brief historical background. This is followed by a summary of the chemical and physical properties of mercury and the compounds it commonly appears in. The environmental cycling of mercury is described followed by the main sources of mercury pollution. The effect of this pollution on the environment, wildlife and human health conclude this section to motivate why decontamination techniques are of high importance.

2.1.1 History of mercury

The name mercury comes from the Roman god of the same name, the messenger of the gods [3]. A fitting name given that mercury has high mobility and surface tension causing it to form liquid beads that roll on most surfaces. This also earns mercury its older and alternative name, quicksilver. The chemical symbol for mercury, Hg, comes from the Greek hydrargyrum meaning liquid silver. The anthropological history of mercury is long and the properties of the element have been described by both Aristoteles and Pliny the Elder [4]. Inorganic mercury, that is mercury compounds not containing carbon, has been extensively used as medicine in ancient times. For example, different compounds have been used as eye and skin ointment, disinfectant, antiseptic and anti-fungal agents. During the sixteenth century, the Swiss physician Paracelsus used pure mercury and other elements in small doses as a medicine for different ailments. Before that, pure mercury had mainly been used as a strong poison. Mercury also held an important role in alchemy where it,

together with sulphur and salt, was believed to be one of the Earth's three principal substances [3, 5]. Mercury was believed to be the core of all metals and thus able to be turned into all other metals by mixing it with other substances. One of the main goals for European alchemists was to transmute materials into gold. Mixtures with mercury and other substances were one of the methods employed to achieve this goal. Mercury in the form of the naturally occurring ore cinnabar was long used to derive the pigment vermilion serving as an important part of the painter's palette [5]

The use of mercury in industrial times is also varied and has played an important role historically. Mercury has been used in the production of paints that prevent fouling on ship hauls [4]. It has also been used as a component in pesticides used in agriculture. Before the discovery of antibiotics, many sexually transmitted bacterial diseases were deadly and the search for cures was desperate [3]. Mercury, and compounds containing mercury, were used as a treatment for syphilis as far as the early 20^{th} century. The treatment appeared to help some patients but since some cases of syphilis are known to resolve spontaneously it remains unclear if mercury worked as a cure. More recently, mercury has been used in several household items throughout the 20^{th} century. Alkaline batteries, fluorescent light tubes, and thermometers used to contain mercury and in some cases still do. Mercury has also historically had an important role in the production of sodium hydroxide and chlorine by electrolysis of brine. Today its role in the chemical industry is mainly as a catalyst [3, 5]. Due to its tendency to form amalgam with most metals, it has been used to extract precious metals [3]. In some countries mercury is still used in small-scale gold mining and artisanal mining [6]. Amalgam has also had a large role as a filling material in dentistry from the 19^{th} century and into modern days [7].

2.1.2 Physical and Chemical properties

Pure elemental mercury takes the form of a dense silvery-white liquid [4]. Mercury has the atomic number 30 and an atomic mass of 200.59 u. Solid mercury forms a rhombohedral crystal structure with a lattice parameter of $a = 0.29925$ nm. The very low melting point of -38.8 C° means that it is liquid at ambient conditions, a unique property among the elements. This also provides mercury with a number of interesting physical and chemical properties [8]. Liquid mercury has a high surface tension resulting in it not wetting glass. It also has high specific gravity and low electrical resistance. The historic use of mercury in thermometers comes from another property, namely that mercury has a uniform volume of expansion over the whole temperature range of its liquid state. Mercury can exist in the three oxidation states Hg^0, Hg^{1+} and Hg^{2+}
, however, Hg^{1+} is rare and do not contribute to the global mass balance [9]. The elemental, zero-valent form of mercury (Hg^0), can occur in three different forms at idle conditions as a liquid, ($Hg^0(l)$), gas ($Hg^0(g)$) or dissolved in water ($Hg^0(aq)$). Since mercury has a relatively high vapour pressure it will readily go from its liquid face to the gaseous one. The gas concentration in equilibrium with liquid mercury is six magnitudes over the recorded background. Mercury vapour is relatively inert and only sparingly soluble in pure water which leads to a long atmospheric residence

time of the order of 1 year. For more information on the environmental cycling of mercury see section 2.1.3.

Although the way we tend to think about mercury is in its elemental form as a silver-coloured metallic liquid it is not the form it typically takes in nature [4]. Mercury is normally found in the earth's crust in the form of 25 differently mercury-containing minerals of which cinnabar (HgS) is the principal one [8]. Mercury also has the property of dissolving many other metals forming alloys called amalgams [4]. It has been recorded that 76 different metals are soluble in mercury to differing degrees.

2.1.3 Environmental cycling of Mercury

Mercury takes part in a natural bio-geo-chemical cycle where it is released from deep reservoirs by volcanic and geological activity, transported in the atmosphere and deposited to land and ocean [10]. It then cycles through the system until ultimately being deposited in deep ocean sediments. This process is however a slow one and estimates of the lifetime of mercury in the system range from about 3000 years to 10 000 years [10]. Human activity has altered the natural cycle on a massive scale since mercury released into the system through pollution also takes part in the natural cycle increasing the total amount of mercury in transfer at any given time [10]. For information on the sources of mercury pollution, see section 2.1.4. Measurements from remote lake sediment cores show that the current mercury deposition is three to five times higher than in preindustrial times [10].

The mercury that enters the atmosphere from geological sources, anthropological sources such as coal-fired power plants, and evaporates from land and ocean surfaces are in its elemental form, Hg^0 [10]. This is the primary mercury form in the atmosphere where it has a lifetime of about 0.5–1 years [10]. This long lifetime allows transfer over long distances and a mostly even spread globally through the atmosphere. Anthropological sources also release divalent mercury (Hg^{2+}) and mercury bound to particles ($Hg(p)$) [10]. These species have a much shorter lifetime in the atmosphere, on the time scale of days to weeks, owing to a higher water solubility than elemental mercury. This also results in these two forms being the main forms deposited on land and to sea. The shorter lifetime leads to regional deposition in the areas where these forms are emitted. Oxidation to divalent mercury is also the main way the elemental mercury leaves the atmosphere [10].

When Hg^{2+} is deposited to terrestrial areas a portion of the mercury is immediately re-volatilised to the atmosphere in a process called prompt recycling. The rate recycled varies between 5–60% depending on the surface deposited, with a higher percentage recycled in wet or snowy environments. Newly deposited mercury is also more prone to convert to methylmercury [10]. The remaining deposition is incorporated into the soil, slowly reentering the atmosphere over a timescale of centuries to millennia [10]. This mercury is initially preferentially associated with vegetation. Hg^{2+} is deposited to and Incorporated in leaves and then enters the soil seasonally

when the leaves are shed. Over 90% of the terrestrial mercury resides in the soil and is associated with organic matter, where it is bound in reduced sulphur groups [10]. This mercury can then be released back into the atmosphere by reduction to elemental mercury and diffusion or mass transport through the soil. Another way that mercury can reenter the atmosphere is when the organic matter it is bound to is burned, naturally through forest fires or otherwise.

Aquatic cycling of mercury occurs both in fresh-water systems and in the marine environment [10]. Neglecting direct contamination, through point sources, the main pathway for atmospheric mercury to enter freshwater systems are from direct deposition to lake surfaces or through runoff from watersheds [10]. The marine system uses the same process as the freshwater one but the exchange at the ocean surface is thought to be rapid [10]. As in the terrestrial counterpart it is mainly divalent mercury that is deposited. This can then be reduced to elemental mercury and reenter the atmosphere. A small portion is also converted to the more toxic form methyl-mercury [10]. This process is facilitated by some strains of sulphate- and iron-reducing bacteria. Methylation occurs to a higher degree in wetlands, lake sediments, continental shelf regions, estuaries and deep-ocean hydrothermal vents. The concentration of mercury varies between the world's oceans with roughly double the concentration in the Mediterranean and North Atlantic compared to the Pacific Ocean [10]. However, the concentration in most ocean basins has not reached equilibrium with atmospheric input and the concentration is believed to rise over the next several decades.

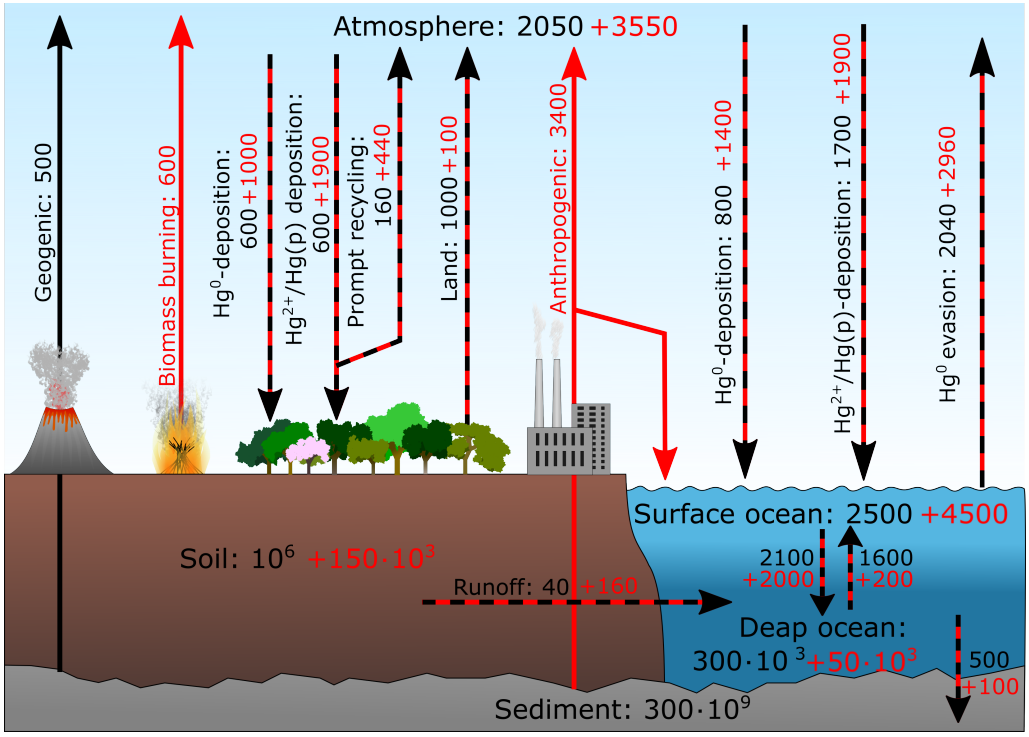

Figure 2.1: Schematic of the environmental cycling of mercury. The amount of mercury in reservoirs is given in tones and mercury transfers in tones/year. Black values denote naturally occurring mercury while red ones denote mercury from anthropological sources. The image is based on an image in an article by N. Selin from which the numerical data is also taken [11].

2.1.4 Sources of mercury pollution

While mercury takes part in a natural cycle of emission into water and atmosphere, and uptake in biomass and sea sediments this is not what we refer to when we talk of mercury pollution. Instead, this refers to the anthropological sources of mercury emission. Since the biogeochemical timescales in the cycling of mercury are on the order of centuries to millennia the human influence on the cycle will have a major impact over the foreseeable future [10]. The current annual anthropological emission of mercury of about 2000 tonnes is more than an order of magnitude above that of natural emissions [12]. The year 1850, taken to be the start of the industrial era, is commonly set as a baseline for mercury emissions. Using lake sediments as an archive of historical mercury deposition we can see that the amount deposited annually has increased by a factor somewhere between 3–5 compared to this baseline [12]. However, this baseline is itself affected by earlier emissions and the increase compared to a true natural level is likely even higher. Streets et al. have estimated the total amount of mercury released to the environment by human activity over all time to be 1540 thousand tonnes [12]. About 73% of this was released after 1850. The largest sources by industrial sector have varied over time as has the geographical distribution. Of the total amount released since 1850 27% come from mercury production, 24% from silver production and 12% from chemical production [12]. During the 19$^{\text{th}}$ century, most air pollution from mercury happened in Europe and

North America but has gradually shifted to Asia, Africa and South America [12]. Before 1850 it is harder to estimate sources but a vast majority stem from silver production, mainly in Spanish America [12].

The 2018 Global Mercury Assessment by UN Environment provide an overview of present-day emissions to air [13]. The by far largest sector, standing for 38% of emissions, is artisanal and small-scale gold mining (ASGM). This is followed by stationary combustion of coal, resulting in 22% of total emissions, and non-ferrous metal production, resulting in 15%. Cement production stands for 11%, disposal of mercury-added product waste 7% and the remaining portion is mainly made up of stationary combustion by other fuels and by ferrous-metal production. Looking at the global distribution of the emissions 39% come from East and Southeast Asia, 18% from South America and 16% from Sub-Saharan Africa [13].

ASGM, being the by far largest source of mercury pollution, warrants a closer look. Although the individual mining operations are typically small the total sector produces between 380–870 metric tons gold a year [14]. For some of the world's largest gold producers ASGM stand for a large amount of the gold output. For example, AGSM make up two-thirds of China's gold production, one-third of Peru's and nearly all of Colombia's [14]. Mercury is inextricably linked with this type of mining as it is used to extract gold from ore and alluvial sediments [14]. The mercury is mixed into milled ore or alluvial sediment to create an amalgam that binds the gold particles and increases the gold recovery rate. Since most ASGM operate at a low technical level a large percentage of the mercury used is released to the environment, either in the form of vapour or as elemental mercury [14]. In addition to direct losses in the amalgamation process, large amounts of mercury accumulate in soil and sediments in connection to this kind of mining operations [13]. This mercury can then re-mobilise and enter aquatic streams. ASGM is typically carried out by single individuals or smaller groups such as families or cooperatives [15]. Many ASGM actors operate illegally without licences making mining practices, including surrounding the use and handling of mercury, lacking in transparency [15]. ASGM is mainly carried out in South America as well as in East and Southeast Asia standing for 53% and 36% of mercury pollution from these sectors respectively [13].

2.1.5 The effect of mercury pollution on wildlife

When looking at the effect of mercury on wildlife from a toxicological perspective it is mainly the highly toxic organic form of mercury, methylmercury (MeHg), that is of interest [16]. The dangers of methylmercury are threefold; it bio-accumulates at the base of the food chain and can bio-magnify at higher trophic levels, it is readily absorbed from the diet to be distributed into many of the body's organs, and it is highly toxic [16]. Bio-accumulation in low trophic organisms, such as algae and microbes, is indicated to be the single largest steep in the increase of MeHg levels with increases 10^4-fold and even higher [17]. For example typical arctic water levels of 10^{-7}–10^{-8} ppm MeHg increase to 10^{-2}–10^{-3} ppm MeHg through bio-accumulation in algae and seston [18]. These levels are then further increased by bio-magnification

to 10^{-2}–10^{-1} ppm MeHg in zooplankton and invertebrates and again to 10^{-1}–10^{0} ppm MeHg in fish. At the top of the food chain apex predators, such as polar bears and predatory birds, can reach levels above 10 ppm MeHg. Toothed whales seem to be especially vulnerable and have been found with high mercury concentration in brain tissue and signs of associated neurochemical effects [17]. Generally, bio-accumulation and bio-magnification of mercury is a larger problem in aquatic environments compared to terrestrial ones, owning to lower baseline levels and shorter food chains [17]. However high levels have been measured in terrestrial species that are indirectly or partly connected to aquatic food chains.

The effects of heightened methyl-mercury in wildlife are many and differ between species. In mammals the toxic effects of MeHg mainly manifest as central nervous system damage with symptoms such as sensory and motor deficits as well as behavioural impairment [16, 19]. Initial symptoms include the animal growing anorexic and lethargic. This is followed by muscle ataxia, motor control deficits, visual impairment and convulsions before death. MeHg can be transmitted from mother to fetus since it is transferable across the placenta [16, 19]. Studies show that MeHg concentrates selectively in the fetal brain and fetal red blood cells contain 30% higher levels MeHg compared to the blood cells of the mother. Twice as high levels MeHg have also been observed in the fetal brain tissue compared to that of the maternal brain [19]. Effects of MeHg exposure during the gestation period range from developmental alterations in the fetus, with resulting deficits after birth, to death of the fetus. Birds are affected much in the same way as mammals but seem to be more prone to reproduction disturbances [19]. These include reduced hatchability, eggshell thinning, reduced clutch size, and an increase in the number of eggs laid outside of the nest. The overall success in reproduction has been shown to decrease between 35% and 50% even at MeHg levels insufficient to cause obvious intoxication in adult individuals [19]. High Hg blood levels in birds have been shown to have several adverse effects on breeding in general ranging from reduced fledgling success to skipped breeding and abnormal reproductive hormone responses [16].

2.1.6 Effects of mercury exposure to human health

Mercury poses a real threat to humans and is identified as the second worst toxic pollution threat to human health by the Blacksmith Institute [20]. Elemental and inorganic mercury mainly pose occupational hazards for those employed in industries that handle mercury [13]. For example, people involved in the production of mercury-containing products, and miners employed in small-scale and artisanal gold mining are at risk [17, 21]. Other exposure paths include amalgam tooth fillings and mercury-containing skin-lightening cosmetic products [17]. Elemental mercury mainly enters the human body through inhalation of mercury vapour [17, 21]. The inhaled mercury enters the bloodstream from where it can enter most tissues of the body and has no problem crossing the blood-brain barrier [17, 21]. After entering the brain it affects the central nervous system with a large number of neurological effects[17, 21].

As discussed in section 2.1.5 methylmercury is the mercury form posing the largest threat to wildlife, and the same is true for human populations [17, 22]. Unlike elemental mercury, the main pathway into the human body for MeHg is ingestion, primarily of contaminated fish and seafood [17, 21, 22]. However, in some regions, high consumption of contaminated rice is instead the main source of exposure [17]. Approximately 90–95% of ingested MeHg is taken up in the bloodstream and gets distributed in the body [17]. About 10% of this MeHg then crosses the blood-brain barrier and gets stored in the brain [17]. MeHg-poisoning in humans causes lysis of cells in the central nervous system with resulting irreversible damage [11, 21, 22]. Symptoms include difficulty coordinating hand- and foot movements, slurred speech, tremors as well as visual, auditory, sensory and balance disturbances [11, 21, 22]. In severe cases the poisoning can result in loss of consciousness and death [22]. Since MeHg can pass through the placenta from mother to child, and the blood-brain barrier is not yet fully developed until one year of age, fetuses and small children are especially vulnerable to MeHg-poisoning [17, 22]. Cases where the child has been poisoned via their mother eating contaminated food during the pregnancy have resulted, in deafness, blindness, severe developmental problems and conditions resembling cerebral parsley [11, 22].

Several high-profile incidents of mass methylmercury poisoning have occurred, of which the one in Minamata Bay in Japan during the 1950 is probably the most well-known and severe [11, 22]. A chemical factory released approximately 640 kg MeHg into the bay resulting in the poisoning of over 3000 people through ingestion of contaminated fish and seafood [22]. The mortality rate is estimated to have been about 30% and among the victims were about 70 children born with congenital damages due to their mothers getting poisoned during pregnancy [22]. Another notable case occurred in Iraq in the 1970s [11, 17]. People were exposed to high MeHg-levels by eating bread made with grain treated with a fungicide that contained mercury [11, 17]. In total 6530 cases of poisoning were recorded resulting in 459 deaths [17].

2.2 Mercury decontamination techniques

There are several available techniques to remove mercury. In this section, the most common are introduced to provide an overview of the available methods. There is currently no single method capable of fulfilling all possible criteria for every single decontamination situation since all available techniques come with their respective advantages and disadvantages [23]. In practice, multiple techniques are often used in combination to reach the desired water quality in a cost-effective way [23].

2.2.1 Precipitation, coagulation, flocculation and flotation

Precipitation, coagulation, flocculation, and flotation are all techniques that work by separating the mercury from the solution to make it easier to collect. Chemical precipitation constitutes the most used method in industry, due to its low cost and its simple operation [23, 24]. The process consists of adding chemicals that react with the solved mercury to form insoluble precipitates. These can then be separated

by sedimentation or filtration [24]. For the treatment of heavy metal ions, such as Hg^{2+}, sulphide precipitation is a common method [24, 25]. Soluble sulphides are added to the wastewater, under weak alkaline conditions, resulting in the precipitation of mercury sulphides [25]. In addition to low cost, high efficiency and easy operation the method can handle high pollutant loads [23, 25]. There are however some disadvantages. Precipitation has low selectivity, resulting in large amounts of toxic sludge in applications with multiple pollutants [23, 25]. In some cases, for example, sulphide precipitation, the added chemical leads to secondary pollution since a large surplus of it is needed [25]. The method is also highly pH dependent and ineffective at low metal ion concentration which limits the possible use cases [23].

Coagulation works by adding a coagulant that forces small insoluble particles called colloids to form larger clusters [24]. The use of coagulants is common in wastewater treatment, but mainly to remove hydrophobic colloids and suspended particles [24]. However, certain coagulants can handle heavy metals as well [24]. Flocculation is an adjacent technique that works by adding flocculants, typically polymers, that cause particles suspended in the wastewater to form larger structures. Since both coagulation and flocculation merely form larger particles they rely on secondary decontamination steps, in the form of, for example, participation or filtration, to remove the pollutants. Both techniques are cost-effective and simple to operate but also share disadvantages in the form of low selectivity, pH dependence and the need of non-reusable chemicals [23].

Instead of causing pollutants to clump together flotation works by making particles attach to gas bubbles that bring them to the surface [24]. This forms a layer of sludge that can then be separated out [24]. Two variants that have been used to handle heavy metals are dissolved air flotation (DAF) and ion flotation [24]. DAF uses microbubbles of air that attach to suspended particles bringing them to the surface [24]. Ion flotation works by letting heavy metal ions, i.e. Hg^{2+}, form hydrophobic species by the use of surfactants [24]. These are then brought to the surface by attachment to air bubbles. Flotation methods are effective at removing small particles and are metal selective [23]. However, they come with high initial capital costs as well as energy costs for operation [23]. The selectivity is also pH dependent limiting use cases [23].

2.2.2 Adsorption

Adsorption is an effective and simple decontamination process that works by letting pollutants adsorb onto surfaces of solid materials [24–28]. Since surface area is directly linked to the adsorption ability of the material porous materials with high surface area are preferred [24–28]. Carbon materials are a common choice, especially activated carbon due to its high micro- and mesopore volume, resulting in high surface area [24–28]. Other carbon structures like carbon nanotubes, mesoporous carbons and graphene have also been used and show great potential [24–27]. To increase the Hg adsorption capacity of materials functional groups, such as sulphur may be added [25–27]. Polymers with incorporated sulphur have been

shown to have a high affinity towards mercury ions [26, 27]. This combined with high surface area results in high adsorption capacity and fast kinetics [26, 27].

Since commercial coal-based activated carbon has risen in price the search for cheaper alternatives has picked up steam [24, 28]. A large number of low-cost adsorbents have been researched including agricultural waste and industrial byproducts, such as fly ash [24–27]. Bio-adsorbents are also an inexpensive and highly effective alternative and come in three categories: non-living biomass, algal biomass and microbial biomass [24]. Non-living biomass can either be of plant or animal origin and the long list of possible materials includes potato peels, sawdust, eggshells, coffee husks, bark, crab shells, animal bones and rice husks [24, 27, 28]. Both algae and microbial adsorbents have also shown promising results and make up renewable and easily grown alternatives [24, 27]. The main downside to bio-adsorbents is that they are hard to regenerate [24].

The advantages and disadvantages of adsorption as a technique for wastewater treatment is highly dependent of the adsorption material chosen [23, 25]. For example, some materials are mercury selective while others have low selectivity and work as global eliminators, i.e. activated carbon [23]. In general, adsorption is a simple and cost-effective process, having a high adsorption rate and low levels of secondary pollution [23, 25]. On the negative side comes the handling of spent adsorption material that may clog or saturate rapidly [23, 25]. Regeneration is possible for some materials but it is often a costly process that involves loss of material [23].

2.2.3 Membrane filtration

Membrane filtration, as the name suggests, relies on liquids passing different kinds of membrane filters that capture pollutants [24]. Several studies where different membrane filters have been used have shown excellent results in removing mercury ions from solution [24, 25, 28]. Four main types of membrane filtration can be used for heavy metal decontamination: ultrafiltration, reverse osmosis, nanofiltration and electrodialysis [24, 25]. Ultrafiltration is a low-pressure filtration technique that is used to remove dissolved and colloidal pollutants [24]. While the pore size of the ultrafiltration filters is larger than dissolved metal ions there are variants of the technique that can handle the smaller pollutant size. Micellar enhanced ultrafiltration (MEUF) work by adding surfactants to the wastewater [24]. These then form micelles that can bind metal ions resulting in structures large enough to be caught by ultrafiltration. Polymer-enhanced ultrafiltration (PEUF) work similarly, but instead of surfactants water-soluble polymers are added to form large complexes with the metal ions, allowing them to be caught in the ultrafiltration [24, 27].

Reverse osmosis is a membrane filtration technique able to remove a wide range of dissolved species [24]. The technique utilises a semi-permeable membrane that lets the purified liquid pass, but not the contaminates [24]. Reverse osmosis has been studied for the removal of heavy metals and demonstrated high removal efficiency [24]. The main drawback comes in the form of high energy consumption to produce

necessary pumping pressure and to regenerate the membrane [24]. Nanofiltration can be seen as an intermediate process between ultrafiltration and reverse osmosis [24]. The technique can be used for heavy metal decontamination and provides simple operation, reliability and comparatively low energy consumption [24]. Studies have indicated that reverse osmosis exhibits slightly better recovery rates while nanofiltration is more suitable for large-scale applications in industry [24].

The last type of membrane filtration is electrodialysis [24]. This process is used to separate ions across charged membranes utilising an electric field as a driving force. The membranes are often ion-exchange membranes, either cation-exchange or anion-exchange. These are described in more detail in section 2.2.4. While electrodialysis has been widely used for desalination of salt-water, salt production and treatment of industrial effluents it has also been proven to be a promising technique for waste-water treatment from heavy metals [24]. Membrane filtration techniques have a number of advantages. The large number of available membranes coupled with small space requirements make a versatile range of applications possible [23, 25]. It is simple, rapid and efficient while producing low levels of solid waste. Depending on the membrane it can also be made metal selective [23, 25]. Amongst the disadvantages, the cost is the primary one making it unavailable for small and medium-sized industries [23, 25]. After high initial investment costs, the process itself also comes with high energy requirements and high costs for maintenance and operation [23, 25].

2.2.4 Ion exchange

Ion exchange techniques are based on reversible chemical reactions where ions in the liquid phase change place with ions in the solid phase in a resin [24, 25]. There are both cation-exchange or anion-exchange resins suitable to handle positive and negative liquid ions respectively [25]. Common cation exchangers are strongly acidic resins with sulfonic acid groups and weakly acidic resins with carboxylic acid groups [24, 25]. In the case of mercury decontamination, the Hg^{2+} ions in the liquid change place with hydrogen ions in the sulfonic or carboxylic groups contained in the ion-exchange resin [24, 25]. the process is affected by several factors including pH, temperature, pollutant concentration, contact time and the ionic charge of the pollutant [24]. In addition to synthetic ion exchange resins, there are natural silicate minerals called natural zeolites capable of good cation-exchange capacity for the removal of heavy metals [24]. Natural zeolites have the added benefit of high abundance and low cost but, unlike synthetic ion exchange resins, their use is still at the laboratory experiment scale [24].

Ion exchange methods have high treatment capacity and since they also are highly efficient for metal removal and exhibit fast kinetics they have become widely used for heavy metal wastewater treatment [23, 24]. This has also led to the availability of a wide array of commercial products, some of which are metal selective [23]. Since the chemical reaction at the heart of ion exchange techniques is reversible, the resins can be regenerated and reused [23, 25]. There is also no secondary pol-

lution associated with the mercury removal process [25]. Among the disadvantages, the aforementioned dependence on pH for optimal performance is worth mentioning along with the need for large columns to handle large streams [23]. Depending on the effluent pre-treatment to remove particulates and organic matter may also be needed [23].

2.2.5 Biological processes

Somewhat adjacent to the biosorbents, biological processes here refer to letting microorganisms or fungi, transform, degrade or adsorb mercury as part of their natural life cycle [25]. While this type of biological treatment is mainly used for organic pollutants some studies have focused on the decontamination of mercury using this type of process [23, 25]. Trials with bacteria, for example, E. coli, in bioreactors have been able to decontaminate wastewater with low mercury concentrations down below people's health requirements [25]. Some seaweeds including brown, green and red algae have been found to have the ability to remove mercury [25]. While environmentally friendly, cheap and highly selective the method is not suitable for higher concentrations of mercury in industrial settings. The need to create a favourable environment for the biological process also limits possible applications and often necessitates significant pre-treatment and continuous monitoring of conditions for situations where the technique is applicable [23, 25].

2.2.6 Electrochemical treatment

This is the category to which the novel decontamination approach that is the subject of this thesis belongs. However being central to the whole project it is covered separately and in more detail in section 2.3 and this section instead focuses on other electrochemical treatment methods. Electrocoagulation works by generating coagulates by electrically dissolving aluminium or iron ions from electrodes and has been studied for mercury ion decontamination [24]. Unlike traditional coagulation there is no need for pH control [23]. Electroflotation functions by running water electrolysis resulting in hydrogen and oxygen gas. The small bubbles of gas are then used for the flotation of pollutants [24]. For more information on coagulation and flotation as methods for decontamination, see section 2.2.1. Electrodeposition uses electricity to make metal ions deposit to the electrodes in elemental form [24]. However, this method is mainly used for the recovery of precious metals and not the decontamination of heavy metals [24].

2.3 Electrochemical alloy formation as a means to remove mercury

This section is about the mercury decontamination method that has been further studied in this thesis and is based on electrochemical alloy formation. First, the basic working principle for the method is presented followed by a section comparing it to the previously described techniques.

2.3.1 Working principle and basic operation

The method is based on electrochemical alloy formation between the mercury ions in solution and a solid platinum electrode [2]. Since amalgamation require interaction between metallic mercury and platinum the ions (Hg^{2+})need to be reduced to metallic mercury (Hg^0) [2]. This can be achieved electrochemically by applying a negative potential to the platinum electrode allowing mercury to reduce at its surface [2]. The elemental mercury is then able to form an amalgam with the platinum. Every platinum atom can bind up to four mercury atoms forming the alloy $PtHg_4$ [2]. The amalgamation process is hindered by low solubility between the two metals at ambient conditions but this can also be mediated electronically. The negative potential applied to the platinum electrode increases the saturation solubility effectively driving the alloy formation [2]. For more detailed technical information on the platinum-mercury system and the alloy formation, see section 3.4. While the formed alloy is stable on the electrode surface, the platinum electrode can be regenerated [2]. By applying a positive potential to the electrode the alloy formation is reversed and the mercury is released to the solution in the form of ions [2]. The ions can be released to a relatively small volume of solution resulting in a small amount of waste [2].

2.3.2 Advantages compared to conventional methods

As seen in section 2.2 there are several decontamination techniques on the market. These however come with their pros and cons that make them hard or prohibitively expensive to employ for certain applications. Studies of the present alloy formation method have shown that the technique is effective for a wide range of mercury ion concentrations [2, 29]. Crucially it can remove mercury down below the safety limits for drinking water and to, or possibly below, typical levels for natural waters [2, 29]. The process is pH independent with regard to the treated solution, which is a notable advantage over many other methods where the monitoring of the pH level is a major drawback [2]. It has even been shown that the method can be used to remove mercury from contaminated concentrated sulphuric acid from a zinc smelter down to levels passing the limits set for high-quality acid [30]. At present there exists no viable commercial mercury removal technique capable of operating at such highly acidic conditions [30]. Unlike the majority of the methods previously discussed this method do not rely on the addition of chemicals or extractants eliminating the need to separate insoluble compounds [2]. The regeneration of the platinum electrode is indicated to be effective and does not generate any waste aside from the small volume of solution into which the mercury is released [2]. The electrochemical removal technique has been shown to work in the presence of calcium, cadmium, copper, iron, magnesium, manganese, sodium, nickel, lead, zinc, and chloride ions allowing for the treatment of chemically complex streams [2]. This capability was also demonstrated in the aforementioned treatment of real-life industrial waste in the form of concentrated sulphuric acid from a zinc-smelter [30]. High selectivity for mercury and low energy requirement further contribute to the potential for this method to be developed into a versatile and attractive mercury decontamination alternative [2, 29, 30].

3

Theory

This chapter contains the necessary theoretical background needed to understand the experimental methods employed in this thesis work. The chapter opens with an introduction to electrochemistry with a closer look at the parts of this field that are central to the experimental part of the thesis. This is followed by theory surrounding the measurement techniques and analysis methods used. The chapter then concludes with previous research and a closer look at the alloy formation process that is at the heart of the studied decontamination method.

3.1 Electrochemestry

Electrochemistry is that branch in chemical physics that describes the connection between electricity and chemical processes. More precisely, it is the study of electron movements in oxidation or reduction at polarised electrode surfaces [31]. In this section, these redox reactions are described and explained. The three-electrode system which serves an integral part in the experimental setup is introduced along with necessary knowledge about potential scales. The section concludes with a look at the reversibility of electrochemical reactions.

3.1.1 Redox reactions and the electrochemical cell

As already mentioned the transfer of electrons via redox reactions is central to electrochemistry [32]. When studying redox reactions it is often easier to separate the reaction into an oxidation part and a reduction part [32, 33]. This allows for separate balancing of the two half-reactions and a better overview of the electron transfer [32, 33]. The two half-reactions are said to form a redox couple [32, 33]. Peter Atkins and Loretta Jones use the reaction between permanganate ions, $MnO_4{}^-$, and oxalic acid, $H_2C_2O_4$, in an acidic solution to illustrate a balanced redox couple in *Chemical Principles: The Quest for Insight* [32]. The balanced pair become

$$\begin{aligned} 2\,MnO_4{}^- + 16\,H^+ + 10\,e^- &\longrightarrow 2\,Mn^{2+} + 8\,H_2O \\ 5\,H_2C_2O_4 &\longrightarrow 10\,CO_2 + 10\,H^+ + 10\,e^-, \end{aligned}$$

where the first reaction is the reduction and the second the oxidation. As can be seen, the electrons are balanced between the reactions and match up to the changes in oxidation number of the oxidised respectively reduced elements. It is here important to note that the splitting of the equation is only a conceptual help since the electrons are never truly free.

In a two-electrode setup, the oxidation takes place at the anode and the reduction at the cathode [32, 33]. The electrodes are connected allowing for a current to be passed between them. The circuit is then closed by placing the electrodes in contact with one or more electrolytes, which facilitates the electron transfer. In other words, the electrodes are placed in ionic contact since ions in the electrolytes can freely transfer electrons between the cathode and the anode [32, 33]. This closed circuit is called an electrochemical cell [32, 33]. Some electrochemical reactions are spontaneous and will produce an electric current simply by closing the circuit, i.e. lithium-ion cells in batteries. These are called galvanic cells [32, 33]. Other redox reactions, such as the one in the decontamination method studied in the thesis, need a supplied current to take place. Electrochemical cells where a non-spontaneous reaction is made possible, by the supply of electrical energy, are called electrolytic cells [32, 33]. This can also be viewed as the reverse reaction is spontaneous. The energy stored in a galvanic cell, or needed to drive an electrolytic cell, is determined by the cell potential [32, 33]. A galvanic cell has a positive cell potential, an electrolytic cell negative potential, and a cell at equilibrium 0 potential [32]. The cell potential can be related to the change in Gibbs free energy between reactants and products of the redox-reaction [32]. Gibbs free energy is the maximum non-expansive work a reaction can do at constant temperature and pressure[32]. This can be expressed as:

$$\Delta G = -nFE_{cell}, \tag{3.1}$$

where ΔG is the change in Gibbs free energy, n the number of transferred electrons, F the Faraday constant, and E_{cell} the cell potential [32]. As seen here the cell potential can be viewed as a criterion of spontaneity. A positive potential relates to a reaction where the Gibbs free energy is decreased, i.e. a spontaneous reaction, and vice versa [32]. It should be noted that applying the cell potential is generally not enough to drive an electrolytic cell and an over-potential that is dependent on the electrode type is generally needed [32].

3.1.2 Standard potentials and three electrode systems

Since there are thousands of possible combinations of electrodes, resulting in different cell potentials, it is convenient to introduce standard potentials for individual electrodes under the standard conditions where all solutes are at 1 $\mathrm{mol} \cdot \mathrm{L}^{-1}$, all gases at 1 atm, and a temperature of 25 °C [32]. The cell potential can thus be written as:

$$E^0_{cell} = E^0_R - E^0_L, \tag{3.2}$$

where E^0_R and E^0_L are the standard potentials of the left and right electrode in the cell diagram respectively, and E^0_{cell} are the cell potential under the same conditions [32]. However, since potentials always describe an energy difference it is impossible to write down the standard potentials of individual electrodes without relating them to a baseline. For this reason, the standard hydrogen electrode (SHE) has been adopted as the universal baseline and arbitrarily set to 0 for all temperatures, i.e.

$$2\,\mathrm{H^+(aq)} + 2\,\mathrm{e^-} \rightleftharpoons \mathrm{H_2(g)} \qquad\qquad E^0 = 0 \text{ V vs. SHE}, \tag{3.3}$$

when working in the SHE potential scale. It should be noted that when referring to SHE the sign of the potential no longer relates to the spontaneity of the reaction under standard conditions, but rather the tendency of the reaction to occur relative to the reduction of hydrogen ions in an ideal solution [32]. All values of potentials in this report are given versus SHE unless otherwise stated [32].

The introduction of a potential scale does not facilitate the practical measurements of potential differences between a single electrode and the electrolyte [34]. To make this possible a physical reference point to measure against is needed; i.e. a reference electrode with a known potential. One could use a SHE reference consisting of a Pt black electrode in 1 M HCl solution over which H_2 gas is bubbled but this is in most cases inconvenient [34]. Several different reference electrodes suitable for different applications are available. In the experimental part of this thesis a Ag/AgCl-reference is used. This consists of a Ag wire that is coated in a porous AgCl-layer and immersed in a 3.0 M KCl solution [33, 34]. The chemical equilibrium in this reference electrode can be written as:

$$\mathrm{AgCl(s) + e^- \rightleftharpoons Ag(s) + Cl^-(aq)} \qquad E = 0.21 \text{ V vs. SHE}, \tag{3.4}$$

where we see that we can transfer potentials measured against this reference to the SHE scale by adding 0.21 V [33–35]. The addition of a reference electrode to the two electrodes of the electrochemical cell results in a three-electrode system [33]. In such a system the electrodes are typically labelled working electrode (WE), counter electrode (CE) and reference electrode (RE) [33]. The working electrode is simply the electrode where the reaction of interest takes place. The reference electrode is the point the working electrode potential is measured against while the current passes between the counter electrode and the working electrode [33, 34]. In a two-electrode setup, the counter electrode and reference electrode are the same. In this case the applied potential, E_app can be written as:

$$E_app = E_{WE} - E_{CE/RE} + IR, \tag{3.5}$$

where E_{WE} is the working electrode potential and $E_{CE/RE}$ is the potential of the combined counter and reference electrode [33, 34]. The last term, IR, signifies the electrical resistance in the electrolyte between the two electrodes. Since changes in E_{app} cause unknown changes in IR the ability to control the potential between the two electrodes is lost [34]. There are cases where the IR term is small, or relatively constant, where a two-electrode system can suffice but for most electrochemical experiments a three-electrode system with separate reference and counter electrodes is needed [33, 34]. No current pass through the reference electrode in this case and it provides a stable well-defined potential against which the working electrode potential can be measured and controlled [33, 34]. All current instead flows between the working electrode and the counter. The applied potential can thus be used to control the potential over the working electrode. The expression simply becomes:

$$E_{app} = E_{WE} - E_{RE}, \tag{3.6}$$

where E_{WE} can be controlled since E_{RE} is both fixed and known [33, 34].

3.1.3 Reversibility of electrochemical reactions and the Nernst equation

Since this project's main concern is the regeneration of the used platinum electrodes it is relevant to say something about the reversibility of electrochemical reactions. There are a number of different types of reversibility that are relevant for electrochemical reactions [33]. The first is chemical reversibility and can be exemplified with the reaction cell reaction of the Ag/AgCl-reference electrode described in equation 3.4. The potential difference between the silver wire and platinum electrode in this cell is 0.21 V vs. SHE and when shorted the right arrow reaction takes place. However, with a supplied voltage sufficient to overcome the cell voltage the reaction can be reversed resulting in the left arrow reaction. In other words, reversing the cell current reverses the cell reaction without any new reactions taking place [33]. This is thus a chemically reversible cell. As a comparison one can look at the system $Zn/H^+, {SO_4}^{2-}/Pt$ where the spontaneous cell reaction can be written:

$$Zn + 2\,H^+ \longrightarrow H_2 + Zn^{2+}. \tag{3.7}$$

An attempt to reverse this cell reaction by applying an external potential sufficient to overcome the cell voltage does reverse the current but results in electrolysis of water:

$$2\,H_2O \longrightarrow 2H_2 + O_2. \tag{3.8}$$

Since the reverse reaction does not take place this is an example of a chemically irreversible cell.

The next type of reversibility is thermodynamic reversibility [33]. A process is said to be thermodynamically reversible when an infinitesimal reversal in the driving force causes the process to reverse direction [33]. Since the infinitesimal driving force in essence requires the system to be in equilibrium a thermodynamically reversible process is one where the process path consists of a continuous series of equilibrium states [33]. A chemically reversible cell may approach thermodynamic reversibility in its operation [33]. This led to the term practical reversibility. Since actual thermodynamic reversibility requires infinite time practical reversibility denotes any real process that can be operated in such a way that thermodynamic equations apply under sufficient accuracy [33].

In section 3.1.1 and equation 3.1 the cell potential was related to the change in Gibbs free energy, but it can also be related to the activity of reactants and products via the Nernst equation [32, 33]. A general electrochemical reaction between reactants A and B resulting in products C and D can be written:

$$aA + bB \rightleftharpoons cC + dD, \tag{3.9}$$

where the lowercase letters denote coefficients. For this reaction, the Nernst equation can be written as:

$$E_{cell} = E^0_{cell} + \frac{RT}{nF} \ln \frac{\alpha_A^a \alpha_B^b}{\alpha_C^c \alpha_D^d}, \tag{3.10}$$

where E_{cell} is the cell potential, E^0_{cell} the standard potential of the reaction, R the gas constant, T the temperature, n the number of electrons, F the Faraday constant, and α_A the activity of species A [32, 33]. The activities are in practice often approximated by the concentrations [33]. If a system adheres to the Nernst equation it is generally dreamed practically reversible and often just called thermodynamically reversible [33].

3.2 Experimental techniques and analysis methods

In this section, the theory and function behind the experimental methods utilised in the experimental part of the project are given. First electrochemical techniques are covered. These include chronoamperometry, chronopotentiometry, linear sweep voltammetry and cyclic voltammetry. This is followed by a section on foam electrodes, electroplating, and then ICP-MS.

3.2.1 Electrochemical measurements

This section explains a number of electrochemical experimental techniques that all centre around an instrument called a potentiostat. The main function of this instrument is to apply, measure and control potentials across two or more electrodes [33]. Typically it is used in a three-electrode system since the static reference electrode provides a fixed potential to measure against, see section 3.1.2. A common electrochemical experiment performed with a potentiostat is chronoamperometry [33]. The method consists of applying a potential step to the working electrode or, in other words, a constant voltage between the working and counter electrode measured against the reference electrode. Meanwhile, the current necessary to maintain this potential is recorded over time. This provides information about electrochemical processes taking place at the working electrode since these will alter this current. It is also possible to supply a fixed current and record the potential over time. This is called chronopotentiometry.

Another technique is linear sweep voltammetry (LSV) [33]. Here the potential is not held constant, but instead altered linearly over time, while the current is recorded. This can be used for scanning for at which potential certain reactions or phenomena take place. Similarly, cyclic voltammetry (CV) relies on a linear scan between two potentials, but when the higher potential is reached the scan direction is reversed and scanned back to the lower potential [33]. Commonly, multiple cycles are performed sequentially. The recorded current is typically plotted against the potential in a voltammogram. From this oxidation and reduction peaks can be identified giving information about redox reactions taking place over the potential interval for both scan directions.

3.2.2 Foam electrodes

In this project, the working electrode consists of different foam materials coated with platinum. In this section some relevant information on foam electrodes in general and the two materials used in this project in particular. Open-pore foam-type electrodes are three-dimensional materials that come in a number of different materials and with a wide range of pore sizes [36]. The porous cellular structure of the foams gives the material a high specific surface area while allowing fluids to pass through [36]. This combined with the ability to choose materials with high conductivity and foams structural rigidity makes them an excellent choice for support onto which active materials may be coated [36]. A common way to classify the porosity of foam electrodes is by their mean cell size measured in pores per inch (ppi) [37]. In this project, a reticulated vitreous carbon (RVC) foam from ERG Aerospace with a cell size of 60 ppi and a stainless steel foam from Fraunhofer IFAM with a cell size of 30 ppi were used. The RVC foam is a skeletal material with a rigid structure that provides both low electrical and fluid flow resistance [38]. RVC foams are also composed of one of the most chemically inert forms of carbon allowing for highly reactive acid electrolytes [38]. The Fraunhofer foam that was used consists of 316L stainless steel and is produced through powder metallurgical replication [39]. This gives the material good electrical conductivity and corrosion resistance. Both materials are reported to have homogeneous cell size across the whole structure [38, 39].

3.2.3 Physical vapour deposition

Physical vapour deposition (VPD) is a coating technique used to deposit a material on top of another [40]. The material that is to be deposited is first transformed into a gaseous phase, which is then deposited onto a substrate. The transfer can be carried out either through thermal evaporation or an impact process [41]. In thermal evaporation, the temperature of the material is raised to the point of evaporation through e.g. thermal heating, electron beam heating or ion beam heating. Similar results can be achieved through an impact process called sputtering. Instead of relying on evaporation the sputtered material is vaporised by bombardment with energetic particles [41]. The vaporised particles are thus dislodged from the source and sputtered onto the substrate, where they forms a film coating.

3.2.4 Electroplating

Electroplating is another coating technique for material deposition onto a substrate and is one of the most common and simple techniques for applying a metallic coating onto a conductive substrate [42]. The substrate is set up as a cathode in an electrochemical cell and plated through the reduction of metal ions. The metal ions can either be supplied directly from oxidation, by using an anode of the desired metal, or by adding metal salts to the electrolyte. In the latter case, an inert anode is used.

3.2.5 Inductively coupled plasma mass spectrometry

Inductively coupled plasma mass spectrometry (ICP-MS) is an analysis technique for the detection and quantification of trace levels of elements in liquid samples [43]. The instrument consists of six major components: the sample introduction system, inductively coupled plasma (ICP), interface, ion optics, mass analyser and detector [43]. The liquid sample enters the instrument through the introduction system where a peristaltic pump transports it to a nebuliser. The nebuliser turns the liquid sample into a fine aerosol. The sample then enters a spray chamber that filters out larger aerosol droplets, preparing it for the ICP. In the ICP-MS instrument the plasma consists of ionised argon-gas and electrons at high temperature. When the aerosol sample reaches the plasma it is atomised and ionised. The resulting ions are extracted in the interface region and then focused into an ion beam by a set of electrostatic lenses. The ion optics then transfer the sample into the quadrupole mass analyser which separates out ions of a certain mass-charge ratio. Ions of a certain element can thus be separated and quantified by the detector. By scanning over different mass-charge ratios a spectrum containing the amounts of all elements in the sample is produced. ICP-MS come with a large number of attractive advantages including its large analytical range and excellent detection limit down to nmol L^{-1} for most elements [43].

ICP-MS is widely used for the determination of trace levels of metals, including mercury species [44, 45]. However, measurement of mercury has proven difficult due to what is called the mercury memory effect [44]. The effect comes from the tendency of mercury to adhere to the walls of the spray chamber and the tubing in the sample introduction system. The effect is prevalent even at low mercury concentrations and leads to several problems including the persistence of mercury signals after sample analyses, even after reasonable rinse time [44, 46–48]. A number of methods to overcome the memory effect have been suggested including the addition of gold to samples as a stabilisation agent, careful selection of rinsing fluids, and multiple rinse cycles between measurements [46–48]. Since the memory effect limits the possibility of returning to baseline after measuring samples containing mercury, it is common practice to measure series with varying mercury content from lowest mercury concentration to highest. The memory effect from a higher concentration sample can otherwise drown out the true mercury signal from a low concentration sample.

3.3 Previous research

Electrochemical alloy formation on platinum for the purpose of mercury decontamination was first described in an article by Christian Tunsu and Björn Wickman in 2018 [2]. Since then several thesis projects have been carried out studying the technique and these have resulted in a couple of articles. The major findings of the initial and subsequent articles are summarised in this section. The original article focuses on proof of concept by testing out a number of important properties that the authors deem necessary for the technique to be a viable alternative to existing

techniques [2]. Using a flat glass electrode plated with 100 nm platinum attached with a 3 nm titanium adhesion layer as a working electrode they managed to saturate the film building approximately 750 nm of alloy, by applying a potential of 0.16 V vs. SHE. They also validated that mercury retrieval worked at pH levels of 0–6.6 and in the presence of calcium, cadmium, copper, magnesium, manganese, sodium, nickel, lead, zinc, and iron without affecting mercury uptake. Using chronoamperometry data from alloy formation they identified the reduction current to be in the range of 40 μA. Using this as oxidation current an electrode loaded to about 12% of the alloy saturation limit was regenerated, demonstrating that the release of mercury is possible and significantly faster than uptake. The regenerated electrode was also successfully reused for another mercury retrieval cycle. Large surface area electrodes were investigated in the form of electrodes onto which ca. 0.02 g of 50%wt. platinum nanoparticles on carbon black were deposited. This test confirmed that a larger electrode surface gave faster retrieval times with about 20 times faster uptake than exhibited on flat electrodes.

In 2023 Emma Feldt et al. published results from investigations of the temperature and concentration dependence of the alloy formation of $PtHg_4$ [29]. This was done both in batch experiments and using Electrochemical quartz crystal microbalance (EQCM). Somewhat simplified, this technique can be described as the working electrode consisting of a very sensitive scale that allows for continuous measurement of mass. In this case, this allows for real-time monitoring of the mercury uptake. The batch experiments confirmed that the decontamination technique is effective for initial mercury concentration in the range 0.25 to 1000 μgL^{-1} Hg^{2+}. The rate of mercury concentration decrease was higher for lower initial concentration which was attributed to the higher Pt:Hg ratio. The investigation also demonstrated that the lowest starting concentration of 250 $\mu gL^{-1}Hg^{2+}$ could be purified down to 6 ng L^{-1} Hg^{2+}, well below the WHO limit for drinking water. The article uses the concentration data to draw conclusions about the alloy formation mechanism and reaction order. For more information on this, see section 3.4. The EQCM measurements at varying temperatures show an anticipated temperature dependence for the reaction rate that can be described with the Arrhenius equation. This relates the reaction rate constant to temperature and activation energy. Using this Feldt et al. estimated the activation energy of alloy formation to 0.29 eV, somewhat lower than previously reported values. The EQCM data also showed that the formation rate is almost constant when carried out in a constant mercury concentration.

Also in 2023, Vera Roth et al. looked into the mercury removal from concentrated sulphuric acid using the alloy formation technique [30]. The goal was to show that the technique could be used to purify sulphuric acid waste from the mining industry down below certain commercial thresholds. Sulphuric acid is considered technical quality if the mercury content is below 0.30 mg/kg and of high purity grade if the mercury content is below 0.08 mg/kg. Unlike the other experiments, these tests were done with foam electrodes in addition to flat electrodes. Both a stainless steel foam (SS316L) with a mean pore size of 45 ppi from Alantum, Fraunhofer IFAM, and a Duocel reticulated vitreous carbon (RVC) with pore size of 60 ppi from ERG

Aerospace were tested. First flat electrodes of platinum coated on glass were used to validate that the technique can be used in the harsh environment of concentrated sulphuric acid. The test confirmed that decontamination is possible in the concentrated acid and that mercury could be removed below the limits for high-purity grade acid. X-ray diffraction (XRD) was then used to confirm that the alloy $PtHg_4$ had been formed. Tests with SS316L plates as substrate were also done, to test the stability in the acid. This test did not reach the same low levels of mercury in the allocated run time of 120 h but was stable. Tests with the SS316L foam coated with 1–2 μm platinum showed an increase in formation rate with a factor of 10, compared to the flat SS316L plate due to the higher surface area and reached below the high-purity threshold. However, the foam proved to suffer from stability issues in the concentrated acid and leaked a considerable amount of iron during the whole experiment and some platinum right at the start. The RVC foam was also tested as a substrate and coated on one side with 200 nm of platinum. This electrode proved to be stable in the acid but the mercury level in acid levelled out after ca 20 h to a concentration of 0.10 mg/kg, just above the high-purity grade. Experiments with an uncoated RVC electrode show that this will attract mercury while the potential is applied but that almost all this mercury is released when the potentiostat is turned off. The article also contains tests with concentrated sulphuric acid in a 20 L reactor with a platinum-coated SS316L working electrode. This larger-scale reactor performed similarly to the lab-scale setup confirming the scalability of the technique for the first time.

3.4 Electrochemical alloy formation in the Platinum-mercury system

Already in the initial article by Björn Wickman and Christian Tunsu alternatives for the reaction path and potential steps for the alloy formation may take place were presented [2]. $PtHg_4$ is assumed to be the dominant phase and the formation of $PtHg_4$ using the decontamination technique has been confirmed by XRD-analyses [2, 30]. However, in the literature references to the formation of both PtHg and $PtHg_2$ are made and they may occur as intermediate compounds in sub-steps of the overall alloy formation [2]. The overall reaction can be written:

$$\mathrm{Pt(s)} + 4\mathrm{Hg^{2+}(aq)} + 8\mathrm{e^-} \rightleftharpoons \mathrm{PtHg_4(s)}, \tag{3.11}$$

where the right arrow direction is the formation and the left regeneration [2, 29, 30]. Emma Feldt et al. tried to identify the rate-limiting step of the alloy formation and for this reason, divided the formation into three major processes:

1. The adsorption and electrochemical reduction of mercury ions on the platinum surface followed by insertion into the alloy.
2. The diffusion of mercury atoms through the already formed $PtHg_4$-alloy layer.
3. The reaction between mercury and platinum at the alloy-platinum interface.

EQCM measurements showed that the rate of formation is constant over time while the potential is applied. From this information, the authors conclude that step 3 is most likely rate-determining. This also implies that the electrochemical $PtHg_4$

formation from mercury ions in solution shares a very similar reaction mechanism to the solid-state reaction between liquid mercury and platinum.

4

Methods

In this section, the methods making up the experimental part of this thesis are described. The two main experiment types in this are formation experiments and regeneration experiments. The formation here refers to the reduction of Hg-ions and formation of Pt-Hg alloy while regeneration refers to the oxidation of Pt-Hg alloy and release of Hg-ions. First, the different working electrodes and their preparation are described. This is followed by a section on the preparation and mixing of electrolytes and liquid samples. The three-electrode setups used for both types of experiments are then presented. This is followed by the various potentiostat settings and sampling procedures for both formation and regeneration and the chapter is then concluded with a summary of the data analysis.

4.1 Working electrodes

Two different types of electrodes were tested as a part of this thesis. The first is a 5 mm thick foam made of SS316L stainless steel and a cell size of 30 ppi manufactured by Fraunhofer IFAM. This foam was coated by SURPRO GmbH. with a few nm gold as an adhesion layer followed by 1–2 μm platinum. The coated foam was cut into four 40 $\times$ 15 mm strips constituting the four samples used and henceforth denoted SS1–SS4. To provide an electrical contact, as well as a mounting point, SS316L steel rods were driven through the top of the foams and twined with pliers to form a secure connection. These functioned both as wires for connecting the foams as working electrodes and as a mounting aid to suspending the foam at an appropriate level in the electrolyte.

The second foam was a 5 mm thick foam made of reticulated vitreous carbon (RVC) with a cell size of 60 ppi manufactured by ERG Aerospace. This foam was sputter coated on one side with 200 nm platinum, and a few nm gold as an adhesion layer, by physical vapour deposition. Just as with the stainless steel foams, the coated RVC foam was cut into four 40 $\times$ 15 mm strips resulting in four samples henceforth denoted RVC1–RVC4. Since the RVC material is very fragile and tends to crumble under stress another method had to be used to provide the electrical contact. A very thin steel wire was instead carefully threaded through the material at the top of the foam and twined into a loop from which the foam was suspended.

4.2 Electrolyte and acid mixing

Several acids are prepared for use as electrolytes and dilution liquid for samples to be analysed in the ICPMS. Sulphuric acid with added mercury for use as an electrolyte in Pt-Hg alloy formation is prepared by mixing 25 ml 95–97% stock concentrated sulphuric acid, 0.9 mL 1000 ppm mercury stock and diluting to 900 mL with Milli-Q ultra pure water. This results in 900 mL 0.5 M H_2SO_4 with a mercury concentration of 1000 ppb. The electrolyte for regeneration was prepared in a similar way but with a higher-grade sulphuric acid stock. Here 24.48 mL 98% concentrated suprapure H_2SO_4 was diluted to 900 ml with Milli-Q ultra-pure water resulting in 0.5 M sulphuric acid. When preparing samples for the ICPMS these had to be diluted in hydrochloric acid. This dilution liquid was prepared by mixing 75.96 mL 37% HCl stock and diluting to 900 mL. To this 0.18 mL 10 ppm bismuth stock was added resulting in 900 mL 1 M HCl acid with a bismuth concentration of 2 ppb. The bismuth was added as a stable and known constant control sample used to normalise the ICPMS data.

4.3 Three electrode set up

The basic experimental setup consisted of a three-electrode system and was mostly the same for both alloy formation and regeneration, changing out only the electrolyte, working electrode and counter electrode. The whole system was built inside of a fume hood. A three-electrode cell beaker was placed on top of a magnetic stirrer with accompanying magnet placed inside the beaker. Inside the beaker, a three-electrode set-up was built consisting of either a platinum-coated RVC foam or a platinum-coated stainless steel foam as a working electrode (see section 4.1), and an Ag/AgCl (SI Analytics, B3610+) as a reference electrode. A platinum wire was used as CE for all formation experiments while different CE were evaluated for regeneration. These were: a platinum wire, a 40 × 40 mm diamond electrode (DIACHEM, Condias), a titanium wire, and a graphite rod. The beaker was filled with 75 ml electrolyte. For formations on RVC foams, the electrolyte was contaminated with concentrated sulfuric acid from a zinc smelting plant in Kokkola, Finland provided by Boliden. The 75 mL of this acid was for most of the tests spiked with 37 μL 1000 ppm Hg stock. Formation on the stainless steel foams was done with 0.5 M sulphuric acid with 1000 ppb Hg. All regeneration was done in 0.5 M sulphuric acid. The three electrodes were connected to a Gamry Reference 600 potentiostat by the use of alligator clips. Initially, the diamond counter electrode was connected by fastening a small wire to its surface with carbon tape and sealed with hot glue but the alligator clip was found to be more secure since the first method was prone to degrade from contact with the vapours from the acid. All equipment in contact with the electrolyte was cleaned with Millie-Q water multiple times both before and after experiments. The electrochemical cell beaker was also cleaned with 1 M sulphuric acid and rinsed five times with Millie-Q before experiments to ensure no contamination. The working electrodes were rinsed with Mille-Q water multiple times before being stored in test tubes with fresh Millie-Q water between experiments.

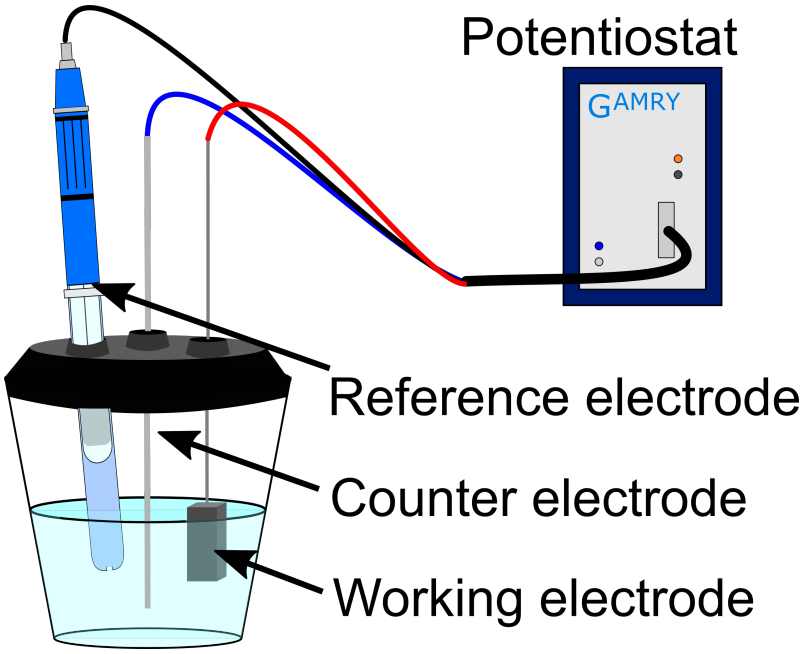

Figure 4.1: A schematic of the three-electrode setup used for both formation and regeneration experiments.

4.4 Potentiostat settings and sampling procedure

The formation was started by applying a potential via linear sweep voltammetry. The sweep is configured from the initial open potential to -0.03 V vs. reference i.e. 0.18 V vs. SHE with a scan rate of 100 mV/s and a step size of 2 mV. This was followed by a chronoamperometry experiment applying the same potential for the remainder of the experiment while recording the applied current. For regeneration, a chronopotentiometry experiment was run by applying a constant current while monitoring the potential instead of controlling it. Two different currents were tested, 20 μA and 40 μA. The duration of experiments varied but in general, the formation experiments were longer and in most cases longer than 24 hours often running over several days. Regeneration was generally carried out over the duration of a working day but in some cases left overnight. The procedure for collecting electrolyte samples for ICPMS analysis was the same for both experiment types. A pipette was used to collect 100 μL electrolyte from the running experiment. This was then diluted by a factor of 50 to 5 ml with 1 M hydrochloric acid containing an internal standard of 2 ppb Bi. When a new experiment was started a initial control sample was taken before any electrodes were introduced and again after introducing the electrode but before any potential or current was applied. In the cases where the electrolyte was spiked an additional control sample was taken after this had been done. The first sample was then taken 10 minutes after the potential or current was applied. The subsequent rate at which samples were collected varied between experiment types. For formation experiments, the electrolyte was sampled about 3 times a day, typically at 10 am, 2 pm and 5 pm. Regeneration was sampled much more frequently with samples taken every 15 minutes, except in those cases when the experiment

was extended to run overnight. At the point of termination, the same procedure was followed for all experiments. The second to last sample was collected before the potentiostat was turned off. The set-up was then left undisturbed with no applied potential or current for 15 minutes before the very last sample was collected.

4.5 Data analysis

The only major data analysis concerns the raw data from the ICPMS analysis. In this section, a brief overview of how this data was processed is provided. The raw data consists of detected counts per second (cps) for all measured elements. By measuring mercury standards with known concentrations of 0, 1, 5, 10 and 50 ppb Hg and Pt a linear regression can be performed for each element to get a formula for converting cps to the desired unit ppb for the respective element. All samples also contain a known internal standard of 2 ppb Bi. Using this the measured data is verified and if needed normalised to eliminate significant errors from sample taking and dilution. The converted concentration is then multiplied by 50 to compensate for the dilution of the samples before analysis. The resulting data is then the measured concentration of Hg and Pt in ppb.

5

Results and discussion

The results with associated interpretation and discussion are presented in this section. First, the evaluation of the counter electrode for regeneration is presented. This is followed by formation and regeneration results from tests with stainless steel foam substrates. An evaluation of two different regeneration currents is also presented and the chapter is closed with results from tests with RVC-foams in concentrated acid from a zink-smelter.

5.1 Evaluation of counter electrode

For mercury decontamination via formation of $PtHg_4$ a platinum wire can be used as a counter electrode. This has been standard in different experiments and proven to provide stable electrical contact. However, it was noticed that platinum was a poor choice of CE for regeneration of the working electrode since the reversed current used to break down the alloy at the WE also drives the formation of Pt-Hg alloy at the CE. This uptake naturally interferes with concentration measurements in the solution since some of the released mercury is taken up by the CE. Similarly subsequent use of the same CE in later WE formation will result in mercury being released from regeneration of the CE. During the experiments, several different CE alternatives have been tested including diamond/carbon plates, titanium wire and graphite rods. The results are somewhat anecdotal stemming from the frequency of connection problems, such as loss of contact during measurements and potential overload. It seems that both the graphite rod CE and titanium wire CE provide good electrical stability comparable to the platinum wire used for formation. Both materials are corrosion-resistant and hold up well in acidic conditions. Neither were tested in the concentrated sulphuric acid but should have worked there too. The diamond/carbon plate that was used for the regeneration in concentrated sulphuric acid had the most frequent connection problems but it is possible that these steamed mainly from problems with connecting the electrode to the potentiostat. First connections were made by using carbon tape to adhere a wire to the plate and then sealing the connection with hot glue. Even though the connection was never in direct contact with the acid capillary action and vapour still resulted in frequent corrosion of the connection. For this reason, this connection method was replaced by connecting the electrode with an alligator clip but the frequent connection problems remained.

5.2 Stainless steel foam substrate

The best results from multiple formation and regeneration cycles stem from tests with $40 \times 15 \times 5$ mm stainless-steel foams (SS316L 30 ppi, Fraunhofer IFAM) electroplated with thin platinum coatings ($< 1\ \mu m$) by SURPRO GmbH. Formation and regeneration experiments are presented in this section.

5.2.1 First cycle

The first cycle refers to the first mercury decontamination, i.e. alloy formation, on a newly coated stainless steel foam followed by subsequent regeneration of the same foam. Here two experiments were running in parallel meaning two foams were going through identical experiments conducted at the same time at two separate but identical experimental setups. Since the results are almost identical, only the results from one of these experiments are presented (SS4) while the results for the other (SS3) are presented in the appendix A.

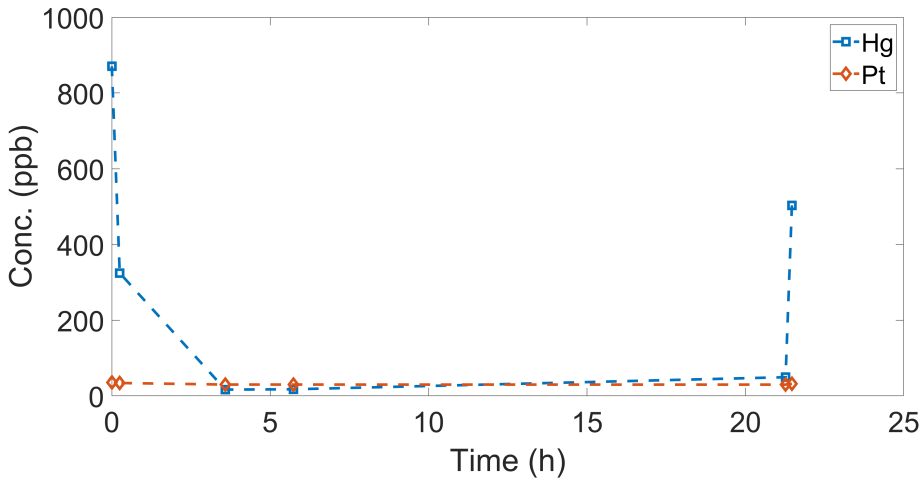

Figure 5.1: ICP-MS data from first alloy formation on foam SS4. Measurements of mercury and platinum concentrations in ppb are shown over a 21:30 hour formation experiment. Note that the formation potential is turned on right after the first measurement and turned off directly after the second to last measurement.

As can be seen in figure 5.1 the first mercury measurement is slightly lower than the expected 1000 ppb at 870 ppb. This first measurement is taken before the potentiostat is turned on but after the foam is introduced. A prior measurement taken of the electrolyte before the foam is introduced has been omitted from the graph for clarity but measured 1059 ppb Hg concentration. This indicates that the foam binds some mercury even before the potential is applied. Since the foam is highly porous giving it a large surface area it is likely that this initial concentration decrease stems from mercury binding to the surface of the material. When the potential is applied the mercury content in the electrolyte is seen to rapidly decrease, lowering to 325 ppb after 15 minutes and have levelled out to 17 ppb at the next measurement taken after 3:35 h. This level is then retained at the next measurement at 5:45 h.

A small, but noteworthy, increase to 49 ppb Hg take place at 21:15 h right before the potential is turned off. This is likely a clear indication of the ICP-MS mercury memory effect since the samples were analysed in reverse order and the last sample had a significantly larger mercury concentration. The memory effect can be seen in most of the experimental data and more information about this effect can be found in section 3.2.5. The true concentration at this point is therefore likely closer to 17 ppb or even lower. Right after this measurement the potential was removed and the foam was left to rest in the electrolyte for 15 minutes before the last sample was taken. This last sample shows a steep increase in the mercury concentration to 503 ppb. About half of the collected mercury is re-released to the electrolyte at this point. It is unlikely that this mercury stems from the decomposition of $PtHg_4$ alloy but rather is metallic mercury collected on the surface of the porous electrode and held in place by the electric potential. When the potential is removed this mercury is almost instantly released back to the electrolyte. It may be hypothesised that this surface mercury will be converted to alloy if the potential is applied over a longer time but longer experiments run over three days show the same behaviour, realising approximately the same amount of mercury when the potential is removed. This indicates that this surface mercury is not available for further alloy formation. No mention of such problems is mentioned by Roth et al. when conducting similar experiments on platinum electroplated stainless steel foams [30]. This might be due to better plating coverage making a larger portion of surface mercury available for alloy formation. It is also conceivable that samples were only taken with applied potential, in which case this issue might be present but undetected. It should be noted that the platinum content in the electrolyte is almost constant over the full experiment and it is unlikely that the foam leaks platinum during alloy formation. The stainless steel foams were stored in Milli-Q water between experiments. Samples were taken of this water after multiple days of storage and showed no significant amounts of either mercury or platinum. It has therefore been assumed that the formed alloy is stable during storage and that all unbounded surface mercury is expelled when the potential is removed.

Following formation, both foams were regenerated by applying a constant current of 20 μA. Foam SS3 used a glassy graphene rod as a counter electrode while SS4 used a titanium wire, otherwise, the setups were once again identical. Since both CE provided stable electrical contacts, and the ICPMS concentration results were very similar only foam SS4 is presented, while the regeneration of SS3 can be seen in Appendix A

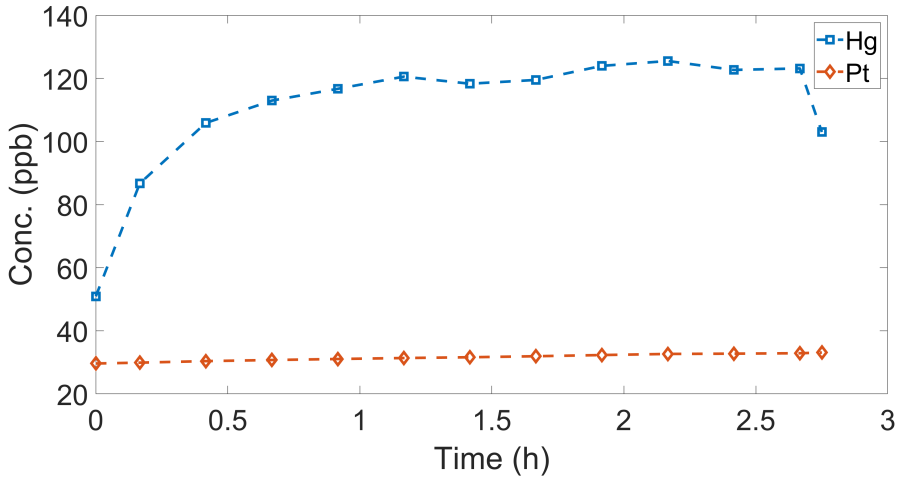

Figure 5.2: ICP-MS data from first regeneration of foam SS4. Note that the regeneration current is turned on right after the first measurement and turned off directly after the second to last measurement.

Just as for the formation a sample of the electrolyte before the foam is introduced has been omitted for clarity. This measured a Hg concentration of 16 ppb and a Pt concentration of 29 ppb. The mercury signal may stem from the mercury memory effect while the Pt signal has an unclear origin. Since the Pt concentration can be observed to be constant over the experiment it can be treated as an offset and it is deemed likely that the platinum on the electrode is stable during the breakdown of $PtHg_4$ for this first cycle. Looking instead at the mercury concentration it is clear that some mercury is released when the foam is introduced to the electrolyte since the mercury concentration increases from 16 ppb to 51 ppb. This is likely mercury trapped in pores and surfaces of the foam made mobile in contact with the electrolyte. It is unlikely that the mercury release taking place before the current is applied is a result of $PtHg_4$ alloy decomposition since earlier tests have shown that the alloy is very stable [2]. From the data can be seen that mercury is rapidly released but at a diminishing rate with a mercury concentration of 87 ppb after 10 minutes and 106 ppb after 25 minutes. After 1:20 h the increase has stooped and the mercury concentration fluctuates around 122 ppb for the remainder of the experiment. The last notable change occurs when the current is turned off after 2:40 h. The sample taken 5 minutes later shows a re-uptake of some mercury with the concentration in the electrolyte going from 123 to 103 ppb. This is likely mercury reattaching itself to the surface of the foam in the absence of the applied current. It is clear from comparing the data from the first alloy formation and subsequent regeneration that not all mercury was released. An amount of mercury corresponding to 502 ppb concentration in the electrolyte was taken up, while only an amount corresponding to 103 ppb was released to the same volume of electrolyte. A possible explanation for the slowing down and eventual halting of mercury release during regeneration can be drawn from the potential data collected during the experiment.

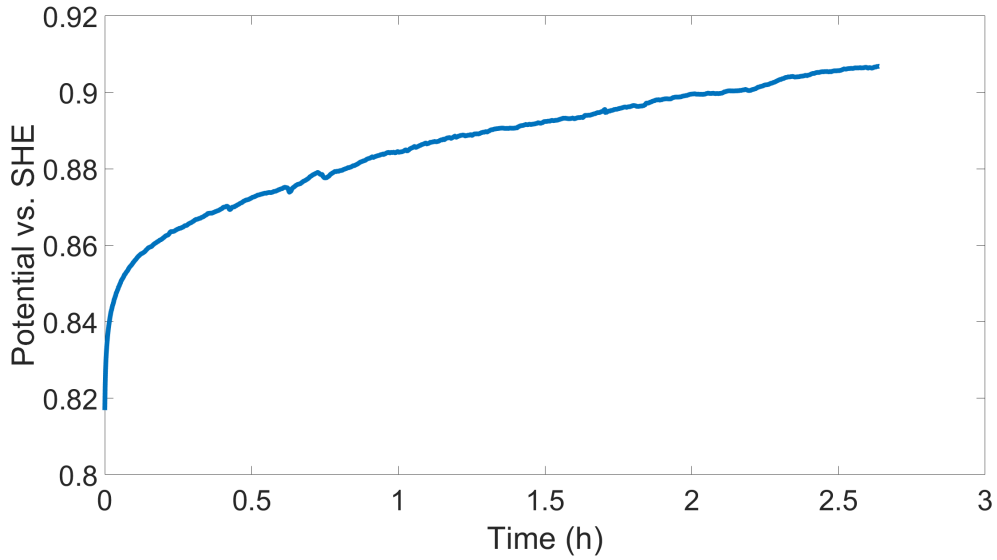

Figure 5.3: Potential data over time for the first regeneration of foam SS4. Corresponding ICP-MS data can be found in figure 5.2.

The potential data reveals a steep increase in the potential during the first minutes of the regeneration, followed by a more linear rise throughout the rest of the experiment. By relating this to the ICP-MS datat it can be observed that when the potential is increased beyond a certain point, the rate of mercury release appears to decrease significantly and eventually level out. Unfortunately, practical circumstances meant that ICP-MS analysis took place a while after the electrochemical measurements, to the effect that this insight could not be used to guide further testing in the scope of this thesis.

5.2.2 Subsequent cycles

Knowing now that the first regeneration was only partially successful subsequent cycles are of less interest than otherwise. It is however still of interest to study the stability and effectiveness. The second formation of foam SS3 and SS4 are once again very similar. The sample taken before the introduction of the foam shows impossibly high values of 1290 ppb for SS3 and 1385 ppb for SS4. Since the electrolyte was mixed with a mercury concentration of 1000 ppb this is odd but has been observed in multiple ICP-MS data sets. While it could be a mixing or sampling error the prevalence of this kind of obvious sampling error across data from multiple experiments with separated setups rather introduce doubt to the accuracy of the ICP-MS analysis. The problem often shows up in experiments carried out on different days but analysed in the ICP-MS at the same time. This in combination with the clear observations of the memory effect puts into question the appropriateness of this analysis method for the mercury samples. Since the ICP-MS analyses were not handled by the author of this thesis the experimentation and resampling needed to find a more accurate procedure were rendered impossible. Ignoring the starting mercury concentration the second formation behaves much like the first. The lowest concentration reached is higher then from the first formation

but it is hard to say if this is accurate since all data from this run may be affected by an offset. Once again the memory effect can be observed on the second to last sample. The most significant information to be collected is that the formation process shows no indication of having been altered when observed on a reused foam.

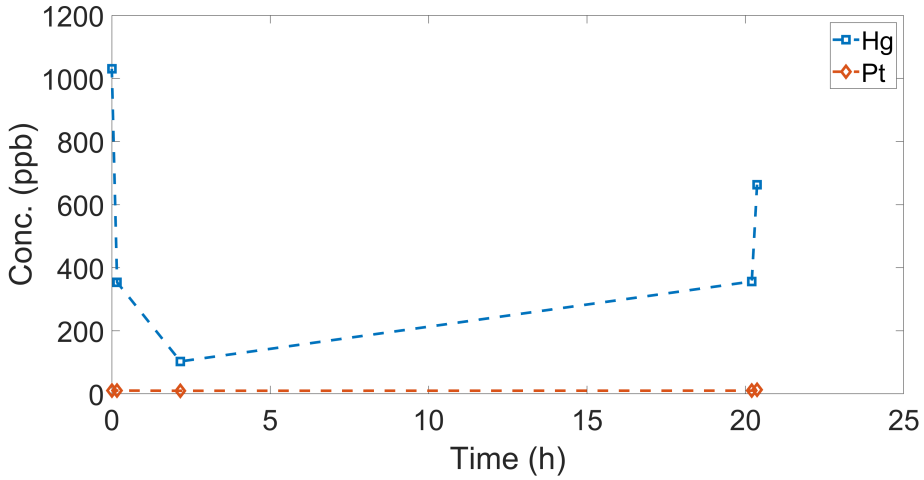

Figure 5.4: ICP-MS data from the second formation of foam SS4. Note that the formation potential is turned on right after the first measurement and turned off directly after the second to last measurement.

The second regeneration of foam ss4 looks very much like the first. An anomaly can be seen at about 2 hours where a sample seems to show a re-uptake of mercury. Since this does not follow the trend and does not show up in the parallel second regeneration of foam SS3 it is deemed an outlier of no importance.

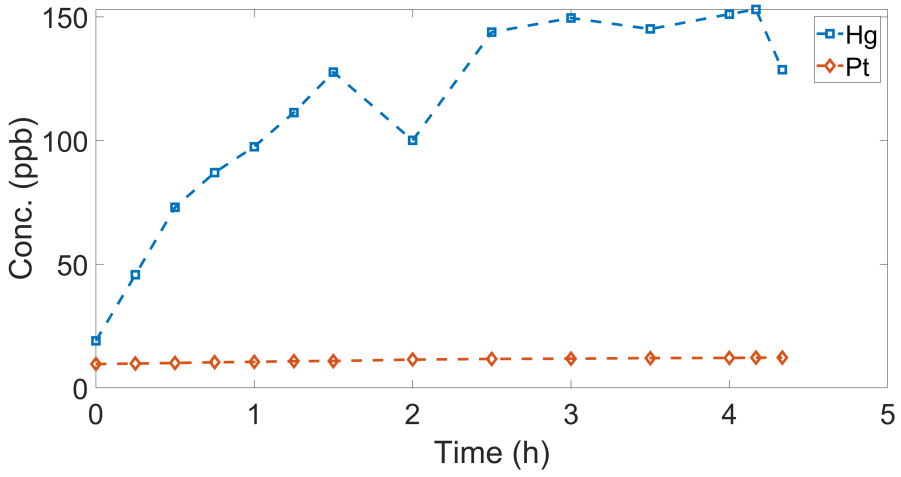

Figure 5.5: ICP-MS data from the second regeneration of foam SS4. Note that the regeneration current is turned on right after the first measurement and turned off directly after the second to last measurement.

The third formation once again show impossibly high mercury concentration for the first samples with the control sample taken before foam introduction measuring 1648

ppb. However, for this formation, very low mercury levels of 17 ppb are reached. Comparing the data of the second and third formation of foam SS4 reveals that the lack of data points unaffected by the memory effect may be the reason why mercury levels in the low tens are not seen. The last sample taken after the potentiostat is turned off also depicts a larger mercury release of 989 ppb. The elevated start levels however make it hard to judge if this constitutes a significant change from previous tests.

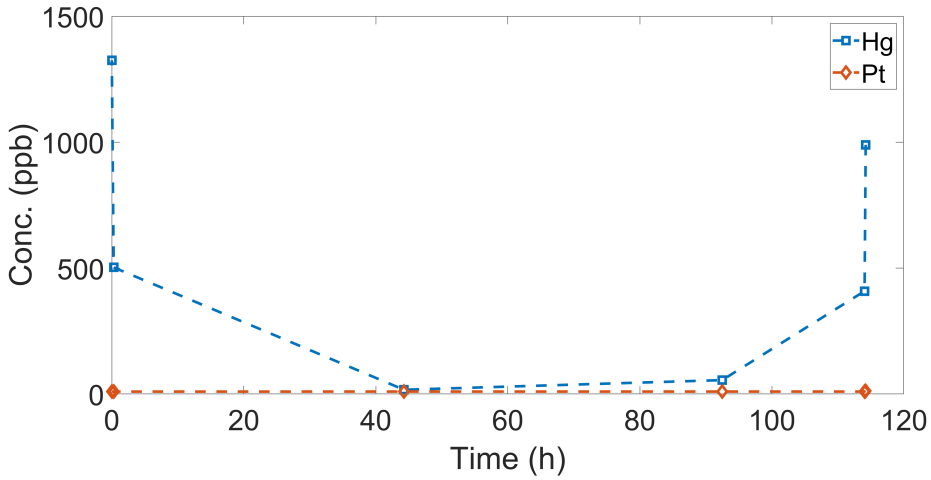

Figure 5.6: ICP-MS data from the third formation on foam SS4. Note that the formation potential is turned on right after the first measurement and turned off directly after the second to last measurement.

The third and last regeneration on foam SS4 does initially look like the rest with a mercury release of about 150 ppb the first hour followed by a leveling out. However, for this regeneration, a slow uptake of mercury takes place from about the 1:30 h mark. This can be seen in the third regeneration of both foam SS3 and SS4. SS3 release a higher amount of mercury levelling out at a concentration of around 250 ppb but the rate of uptake is also slightly higher resulting in both experiments measuring about the same mercury concentration at the point of termination. It is hard to draw any conclusions from this given the small sample size but it is not unreasonable to assume that multiple formation/regeneration cycles may alter the behaviour of the electrode due to the drastic restructuring of the platinum layer that the alloy formation constitutes. More research, ideally achieving a more complete regeneration and more cycles would probably showcase if any significant material properties are altered. It is important to note that almost no change in the platinum levels in the electrolyte is observed in any of these formation or regeneration experiments indicating a stable adhesion to the foam and stability over the alloy formation and decomposition process.

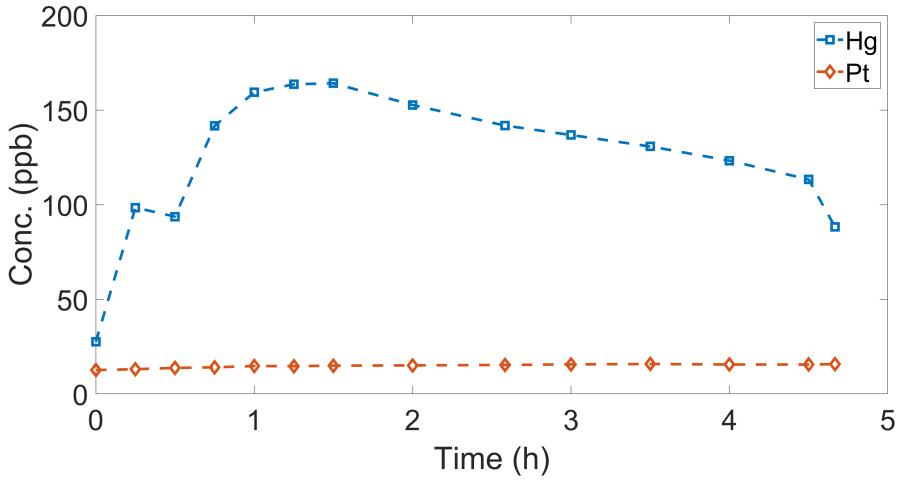

Figure 5.7: ICP-MS data from the third regeneration of foam SS4. Note that the regeneration current is turned on right after the first measurement and turned off directly after the second to last measurement.

5.3 Evaluation of regeneration current

Foams SS1 and SS2 behave much like SS3 and SS4 but with a higher fail rate due to problems with the electrical contact and potentiostat overloads likely owned to the diamond counter electrode being used for most of the regeneration experiments in these cycles. However, SS1 and SS2 were regenerated at different currents, 20 μA and 40 μA respectively, providing some valuable information. Here the third regeneration of both these foams is presented since they both use titanium wire as CE providing stable electrical contact and isolating the current as the only difference between the two experiments.

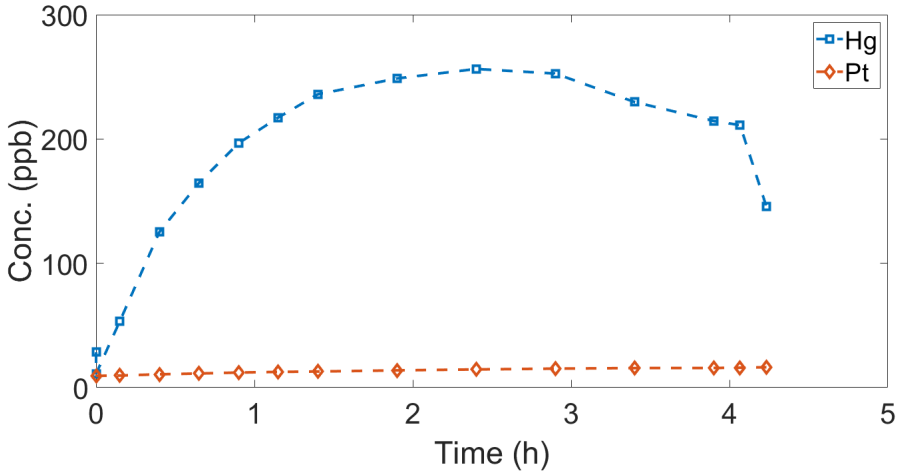

Figure 5.8: ICP-MS data from the third regeneration of foam SS1. Note that this regeneration was carried out with a 20 μA applied current. The regeneration current is turned on right after the first measurement and turned off directly after the second to last measurement.

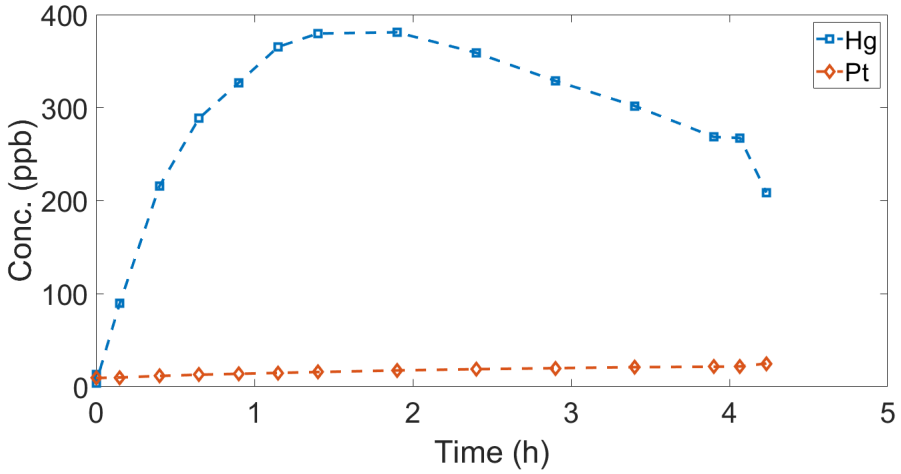

Figure 5.9: ICP-MS data from the third regeneration of foam SS2. Note that this regeneration was carried out with a 40 μA applied current. The regeneration current is turned on right after the first measurement and turned off directly after the second to last measurement.

Comparing figure 5.8 and 5.9 one see that the higher regeneration current results in a larger amount of mercury being released but also a faster and more sudden levelling out of the release. The reuptake of mercury is also more pronounced and starts earlier in the regeneration. The larger amount of mercury being released is expected since the dubbled current result in a more violent and fast oxidation process. The more sudden leveling-off of mercury release is consistent with the earlier observations that the regeneration process becomes less efficient over time. While mercury is released in the initial stages of the process, the rate of release diminishes as the experiment progresses, with a notable slowdown before the reaction appears

to halt. Further investigations would be required to fully understand the factors affecting the regeneration process. Test of this kind is in the author's mind the next logical step for further research on the decontamination technique

5.4 RVC-foam substrate

The tests with Pt-coated RVC foams were plagued by problems with the electrical contact. Given the stability problems it is deemed unreliable to study these foams as consistent over multiple cycles. For example, there are examples where the data seem to indicate that more mercury is released than was taken up. Some individual formations and regeneration however carry interesting results when studied on their own. The very first formation on RVC1 is interesting since it manage to reach very low mercury concentrations in the contaminated concentrated sulphuric acid. Roth et. al. present results from decontamination with platinum sputtered RVC foam and present results where technical quality (0.30 mg/kg) is reached but not high purity (0.08 mg/kg) [30]. Since 1 ppb = 0.001 mg/kg the level reached in figure 5.10 of 76 ppb = 0.076 mg/kg is just below the high purity level and a slight improvement over previously published results. After this formation a decision was made to spike the electrolyte with additional mercury for subsequent formations and owning to this these low levels were not replicated in later formation experiments. It can also be noted that the high level of mercury release observed when the potential is turned off in the formation experiments with the stainless steel foams is not present in observed here.

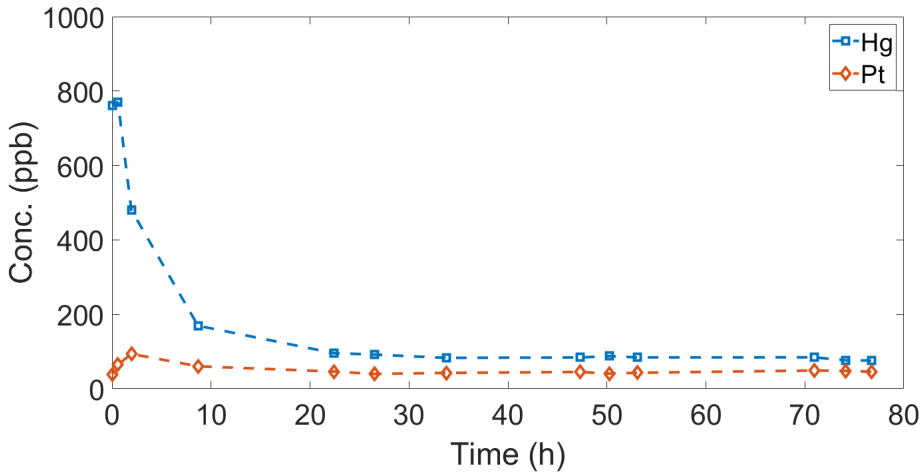

Figure 5.10: ICP-MS data from the first formation of foam RVC1. Note that the formation potential is turned on right after the first measurement and turned off directly after the second to last measurement.

Most regenerations on the RVC foams look like the results presented for the stainless steel with mercury levels corresponding to a few hundred ppb being released before levelling out followed by a re-uptake of mercury. The first formation (figure 5.11) and regeneration (figure 5.12) on the foam RVC2 will serve as a typical cycle without

any obvious anomalies from connection issues. As can be seen the higher mercury content in the spiked concentrated acid leads to levelling out on a higher mercury level of about 210 ppb. Here the lack of any mercury release at the point of turn-off can be seen. This could either be due to that the RVC material does not take up mercury to the same extent as the stainless steel or, more likely, take up mercury but bind it more securely than the stainless steel. Since carbon materials are often used in mercury absorption this seems likely.

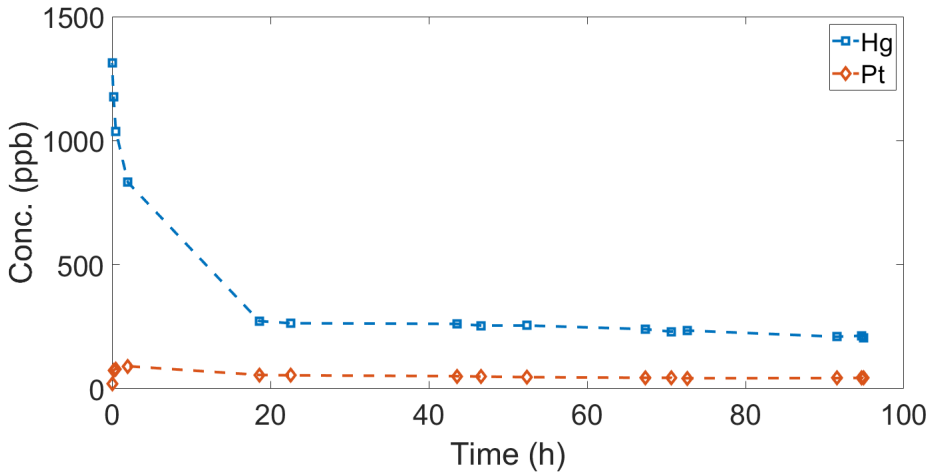

Figure 5.11: ICP-MS data from the first formation of foam RVC2. Note that the formation potential is turned on right after the first measurement and turned off directly after the second to last measurement.

The regeneration of RVC foams exhibits the same behaviour as the stainless steel but instead of levelling out after an initial mercury release the mercury is taken up again at a rate comparable to the initial release rate. Even if the behaviour is somewhat different the same leveling out of the mercury release can be seen in this case also. Interestingly some platinum can be seen to be released during the release and uptake of mercury. While this may indicate some stability problems with the RVC substrate a slower regeneration with a lover regeneration current will probably solve these problems.

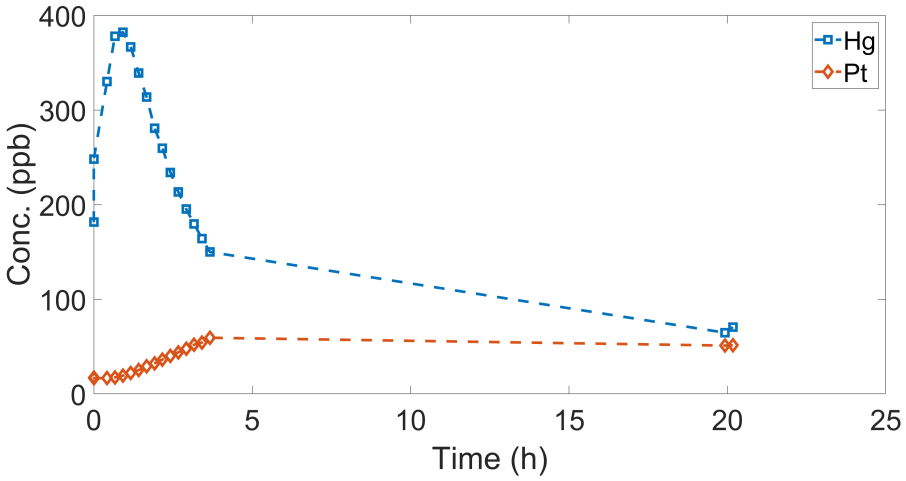

Figure 5.12: ICP-MS data from the first regeneration of foam RVC2. Note that the regeneration current is turned on right after the first measurement and turned off directly after the second to last measurement.

6
Conclusions and Outlook

In this concluding part of the thesis, the major findings and insights from this project are summarised in a conclusion section. Finally an outlook is provided to look ahead at possible next steps in the development of the mercury decontamination technique.

6.1 Conclusions

While the main aim of this thesis was not fully achieved several advances and new realisations have been made. Further regeneration studies should focus on refining the operational parameters to improve mercury release efficiency during the regeneration process. While the incomplete regenerations have hindered a reliable study of the behaviour of the foam electrodes over several complete formation/regeneration cycles it is clear that the foams withstand and retain their decontamination ability after going through several violent, if incomplete regenerations. Since a gentler and slower regeneration process is likely the way forward, these more extreme tests serve as a good test of stability. That no significant loss of platinum is observed for the regeneration tests with stainless steel substrates is a good sign for the future of the project.

The tests with RVC-foams in concentrated sulphuric acid have also improved on previous results demonstrating that the technique can be used to decontaminate concentrated sulphuric down below the commercial threshold for high purity. An important result for future commercial applications of the technique. The slight release of platinum is not seen as a major obstacle since a gentler regeneration method is likely to lead to higher platinum stability. RVC-substrates are in addition to the stainless steel therefore seen as a viable way forward for commercial application where the stainless steel can not be used. For example concentrated sulphuric acid.

6.2 Outlook

In this final section, an outlook is provided with suggestions for further research and possible next steps for the development of the mercury decontamination technique. Given the problems outlined in the result section the obvious next step would be to implement the insights gained that were outside the scope of this thesis. While the same methodology used in this thesis could be used armed with the insight that an optimal regeneration current is yet to be discovered it is probably wise to take a step back. The move from flat working electrodes to foams for the alloy formation

part of the process was preceded by extensive research with EQCM measurements to gain an understanding of the alloy formation process. The same is not true for regeneration where the published research consists of preliminary tests providing proof of concept rather than a detailed understanding. EQCM measurements provide continuous monitoring of the bounded mass on flat electrodes in real-time. This instant feedback provides a much greater opportunity to quickly test and compare different regeneration procedures. When a reliable regeneration method has been found, and ideally some insight into the regeneration mechanism gained, further tests on foams can be done with greater confidence. At that point, research into the stability and behaviour of foam electrodes over multiple cycles will be a key part of the further development of the technique for commercial use. Since EQCM can not be used for foam materials the methodology used in this thesis with ICPMS analysis of batch samples just as in this project. As has been seen this method comes with several problems and uncertainties. While a deeper understanding of regeneration eliminates some of these, experimenting with more ways to stabilise the mercury during ICP-MS analysis and thus minimising the memory effect would result in more reliable data. It has also been seen that the electrical contact to the foam has been a concern. The development of a holder with secure electrical contact to the foam would likely eliminate these problems giving a much higher rate of success in experiments and enabling longer cycles of formation/regeneration. A holder was designed as part of this thesis but was never produced or used. The schematics of this is presented in Appendix B

Further tests of RVC-foams in concentrated acid open up many more possible applications for the decontamination technique in industry. While more problems were seen in these tests during this thesis the large possible gain, if this application can be made to work reliably, makes further research into this area very interesting. Having identified multiple sources of problems with possible solutions there remain many things to try that may be the key to making decontamination of concentrated acid a possibility.

While the results from this thesis have highlighted a number of problems it has also illuminated multiple possible ways forward and it is the author's firm belief that they will be overcome with further research.

Bibliography

[1] World Health Organization, *10 Chemicals of Public Health Concern*, 2020. [Online]. Available: https://www.who.int/news-room/photo-story/photo-story-detail/10-chemicals-of-public-health-concern.

[2] C. Tunsu and B. Wickman, "Effective removal of mercury from aqueous streams via electrochemical alloy formation on platinum," *Nature Communications 2018 9:1*, vol. 9, no. 1, pp. 1–9, Nov. 2018, ISSN: 2041-1723. DOI: 10.1038/s41467-018-07300-z. [Online]. Available: https://www.nature.com/articles/s41467-018-07300-z.

[3] J. Sloane, *Mercury: Element of the Ancients | Dartmouth Toxic Metals*. [Online]. Available: https://sites.dartmouth.edu/toxmetal/mercury/mercury-element-of-the-ancients/.

[4] L. F. Kozin and S. C. Hansen, *Mercury Handbook: Chemistry, Applications and Environmental Impact*. Cambridge: The Royal Society of Chemistry, 2013, p. 334, ISBN: 9781849734097.

[5] R. Fortey, *The Earth: An Intimate History*. London: The Folio Society, 2004, p. 210.

[6] M. Schwartz, K. Smits, and T. Phelan, "Quantifying mercury use in artisanal and small-scale gold mining for the Minamata Convention on Mercury's national action plans: Approaches and policy implications," *Environmental Science and Policy*, vol. 141, no. January, pp. 1–10, 2023, ISSN: 18736416. DOI: 10.1016/j.envsci.2022.12.002. [Online]. Available: https://doi.org/10.1016/j.envsci.2022.12.002.

[7] "Composite Resin versus Amalgam for Dental Restorations: A Health Technology Assessmen," CADTH, Ottawa, Tech. Rep. March, 2018.

[8] W. H. Schroeder and J. Munthes, "ATMOSPHERIC MERCURY-AN OVERVIEW," *Atmospheric Environment*, vol. 32, no. 5, pp. 809–822, 1998.

[9] G. Bigham, B. Henry, and B. Bessinger, "Environmental Forensics," in *Environmental Forensics: Contaminant Specific Guide*, R. Morrison and B. Murphy, Eds., Academic Press, 2005, pp. 1–17, ISBN: 9780125077514. DOI: 10.1016/B978-0-12-507751-4.X5021-6. [Online]. Available: https://www.sciencedirect.com/science/article/pii/B978012507751450023%20https://linkinghub.elsevier.com/retrieve/pii/B9780125077514X50216.

[10] N. E. Selin, "Global biogeochemical cycling of mercury: A review," *Annual Review of Environment and Resources*, vol. 34, pp. 43–63, 2009, ISSN: 15435938. DOI: 10.1146/annurev.environ.051308.084314.

[11] N. E. Selin, "Global biogeochemical cycling of mercury: A review," *Annual Review of Environment and Resources*, vol. 34, no. June, pp. 43–63, 2009, ISSN: 15435938. DOI: 10.1146/annurev.environ.051308.084314.

[12] D. G. Streets, H. M. Horowitz, D. J. Jacob, Z. Lu, L. Levin, A. F. Ter Schure, and E. M. Sunderland, "Total Mercury Released to the Environment by Human Activities," *Environmental Science and Technology*, vol. 51, no. 11, pp. 5969–5977, 2017, ISSN: 15205851. DOI: 10.1021/acs.est.7b00451.

[13] "Global Mercury Assessment," Tech. Rep. 3, 2018, pp. 209–212. [Online]. Available: http://www.unep.org/gc/gc22/Document/UNEP-GC22-INF3.pdf.

[14] A. R. Aldous, T. Tear, and L. E. Fernandez, "The global challenge of reducing mercury contamination from artisanal and small-scale gold mining (ASGM): evaluating solutions using generic theories of change," *Ecotoxicology*, 2024, ISSN: 15733017. DOI: 10.1007/s10646-024-02741-3.

[15] Y. Cheng, T. Watari, J. Seccatore, K. Nakajima, K. Nansai, and M. Takaoka, "A review of gold production, mercury consumption, and emission in artisanal and small-scale gold mining (ASGM)," *Resources Policy*, vol. 81, no. February, p. 103 370, 2023, ISSN: 03014207. DOI: 10.1016/j.resourpol.2023.103370. [Online]. Available: https://doi.org/10.1016/j.resourpol.2023.103370.

[16] A. Scheuhammer, B. Braune, H. M. Chan, H. Frouin, A. Krey, R. Letcher, L. Loseto, M. Noël, S. Ostertag, P. Ross, and M. Wayland, "Recent progress on our understanding of the biological effects of mercury in fish and wildlife in the Canadian Arctic," *Science of the Total Environment*, vol. 509-510, pp. 91–103, 2015, ISSN: 18791026. DOI: 10.1016/j.scitotenv.2014.05.142. [Online]. Available: http://dx.doi.org/10.1016/j.scitotenv.2014.05.142.

[17] F. Beckers and J. Rinklebe, "Cycling of mercury in the environment: Sources, fate, and human health implications: A review," *Critical Reviews in Environmental Science and Technology*, vol. 47, no. 9, pp. 693–794, 2017, ISSN: 15476537. DOI: 10.1080/10643389.2017.1326277. [Online]. Available: https://doi.org/10.1080/10643389.2017.1326277.

[18] I. Lehnherr, "Methylmercury biogeochemistry: A review with special reference to Arctic aquatic ecosystems," *Environmental Reviews*, vol. 22, no. 3, pp. 229–243, 2014, ISSN: 12086053. DOI: 10.1139/er-2013-0059.

[19] M. F. Wolfe, S. Schwarzbach, and R. A. Sulaiman, "Effects of mercury on wildlife: A comprehensive review," *Environmental Toxicology and Chemistry*, vol. 17, no. 2, pp. 146–160, 1998, ISSN: 0730-7268. DOI: 10.1002/etc.5620170203.

[20] A. McCartor, D. Becker, D. Hanrahan, B. Ericson, A. Thomen, R. Fuller, D. Jones, and J. Caravanos, "World's Worst Pollution Problems Report 2010," Blacksmith institute, Green Cross Switzerland, Tech. Rep., 2010. [Online]. Available: https://www.greencross.ch/wp-content/uploads/uploads/media/pollution_report_2010_top_six_wwpp.pdf.

[21] N. Kumar, *Mercury Toxicity: Challenges and Solutions*, N. Kumar, Ed. Singapore: Springer Singapore, 2023, ISBN: 978-981-99-7719-2. DOI: 10.1007/978-981-99-7719-2. [Online]. Available: https://link.springer.com/book/10.1007/978-981-99-7719-2.

[22] H. Yokoyama, *Mercury Pollution in Minamata*. Kyoto, Japan: Springer Open, 2018, ISBN: 9789811073922. [Online]. Available: http://www.springernature.com/series/8868.

[23] G. Crini and E. Lichtfouse, "Advantages and disadvantages of techniques used for wastewater treatment," *Environmental Chemistry Letters*, vol. 17, no. 1, pp. 145–155, 2019, ISSN: 16103661. DOI: 10.1007/s10311-018-0785-9. [Online]. Available: https://doi.org/10.1007/s10311-018-0785-9.

[24] F. Fu and Q. Wang, "Removal of heavy metal ions from wastewaters: a review," *Journal of environmental management*, vol. 92, no. 3, pp. 407–418, 2011, ISSN: 1095-8630. DOI: 10.1016/j.jenvman.2010.11.011. [Online]. Available: http://www.ncbi.nlm.nih.gov/pubmed/21138785.

[25] K. Hua, X. Xu, Z. Luo, D. Fang, R. Bao, and J. Yi, "Effective Removal of Mercury Ions in Aqueous Solutions: A Review," *Current Nanoscience*, vol. 16, no. 3, pp. 363–375, 2019, ISSN: 15734137. DOI: 10.2174/1573413715666190112110659.

[26] K. G. Pavithra, P. SundarRajan, P. S. Kumar, and G. Rangasamy, "Mercury sources, contaminations, mercury cycle, detection and treatment techniques: A review," *Chemosphere*, vol. 312, no. P1, p. 137 314, 2023, ISSN: 18791298. DOI: 10.1016/j.chemosphere.2022.137314. [Online]. Available: https://doi.org/10.1016/j.chemosphere.2022.137314.

[27] J. G. Yu, B. Y. Yue, X. W. Wu, Q. Liu, F. P. Jiao, X. Y. Jiang, and X. Q. Chen, "Removal of mercury by adsorption: a review," *Environmental Science and Pollution Research*, vol. 23, no. 6, pp. 5056–5076, 2016, ISSN: 16147499. DOI: 10.1007/s11356-015-5880-x.

[28] A. Sharma, A. Sharma, and R. K. Arya, "Removal of Mercury(II) from Aqueous Solution: A Review of Recent Work," *Separation Science and Technology (Philadelphia)*, vol. 50, no. 9, pp. 1310–1320, 2015, ISSN: 15205754. DOI: 10.1080/01496395.2014.968261. [Online]. Available: http://dx.doi.org/10.1080/01496395.2014.968261.

[29] E. Feldt, J. Järlebark, V. Roth, R. Svensson, P. K. Gustafsson, N. Molander, C. Tunsu, and B. Wickman, "Temperature and concentration dependence of the electrochemical PtHg4 alloy formation for mercury decontamination," *Separation and Purification Technology*, vol. 319, no. May, 2023, ISSN: 18733794. DOI: 10.1016/j.seppur.2023.124033.

[30] V. Roth, J. Järlebark, A. Ahrnens, J. Nyberg, J. Salminen, T. R. Vollmer, and B. Wickman, "Mercury Removal from Concentrated Sulfuric Acid by Electrochemical Alloy Formation on Platinum," *ACS ES and T Engineering*, vol. 3, no. 6, pp. 823–830, 2023, ISSN: 26900645. DOI: 10.1021/acsestengg.2c00417.

[31] B. A. Patel, *Electrochemistry for Bioanalysis*. Elsevier Inc., 2021, pp. 1–8. DOI: 10.1016/c2019-0-03108-1.

[32] P. Atkins and L. Jones, *Chemical Principles: A Quest for Insight*, 5th. New York: W. H. Freeman and Company, 2010, p. 392, ISBN: 9781429219556.

[33] A. J. Bard and L. R. Faulkner, *ELECTROCHEMICAL METHODS Fundamentals and Applications*, 2nd. Austin, Texas: John Wiley & Sons, Inc, 2001, ISBN: 0471043729.

[34] R. G. Compton and C. E. Banks, *Understanding Voltammetry*, 3ed. Singapore: World Scientific Publishing Europe Ltd., 2018, p. 439, ISBN: 9781786345264.

[35] E. Lechner M.D., R. Holze, and E.-C. Martienssen W., "Table 1.6. Potentials of common reference electrodes in aqueous solution.," in *Electrochemical Thermodynamics and Kinetics*, Berlin: Springer, 2007, p. 75. [Online]. Available: https://search.ebscohost.com/login.aspx?direct=true&db=edssmt&AN=springer.978.3.540.45316.1.Chapter.8&site=eds-live&scope=site&authtype=guest&custid=s3911979&groupid=main&profile=eds.

[36] W. Zheng, M. Liu, and L. Y. S. Lee, "Best Practices in Using Foam-Type Electrodes for Electrocatalytic Performance Benchmark," *ACS Energy Letters*, vol. 5, no. 10, pp. 3260–3264, 2020, ISSN: 23808195. DOI: 10.1021/acsenergylett.0c01958.

[37] J. Standke Gisela; Adler, "Open-Celled Silicon carbide foams made by replication method – Manufacturing, properties and application of SSIC and SISIC Foams," *Intern. Conf. on Porous Ceramic Materials*, no. figure 1, pp. 1–6, 2005.

[38] ERG, *Carbon (RVC) Foam*. [Online]. Available: https://ergaerospace.com/carbon-rvc-foam-open-cell-material/.

[39] P. Quadbeck, "Open cell metal foams," *Fraunhofer institute for manufacturing technology and advanced materials IFAM, Branch lab Dresden*, pp. 4–5, 2016. [Online]. Available: http://www.ifam.fraunhofer.de/content/dam/ifam/en/documents/dd/Infobl%C3%A4tter/open_cell_metal_foams_fraunhofer_ifam_dresden.pdf.

[40] A. Makhlouf, "Current and advanced coating technologies for industrial applications," *Nanocoatings and Ultra-Thin Films*, pp. 3–23, Jan. 2011. DOI: 10.1533/9780857094902.1.3.

[41] K. Reichelt and X. Jiang, "The preparation of thin films by physical vapour deposition methods," *Thin Solid Films*, vol. 191, no. 1, pp. 91–126, 1990, ISSN: 00406090. DOI: 10.1016/0040-6090(90)90277-K.

[42] A. Yli-Pentti, "Electroplating and Electroless Plating," *Comprehensive Materials Processing: Thirteen Volume Set*, vol. 4, pp. 277–306, Jan. 2014. DOI: 10.1016/B978-0-08-096532-1.00413-1.

[43] S. C. Wilschefski and M. R. Baxter, "Inductively Coupled Plasma Mass Spectrometry: Introduction to Analytical Aspects," *Clinical Biochemist Reviews*, vol. 40, no. 3, pp. 115–133, 2019, ISSN: 18380212. DOI: 10.33176/AACB-19-00024.

[44] Y. Li, C. Chen, B. Li, J. Sun, J. Wang, Y. Gao, Y. Zhao, and Z. Chai, "Elimination efficiency of different reagents for the memory effect of mercury using ICP-MS," *Journal of Analytical Atomic Spectrometry*, vol. 21, no. 1, pp. 94–96, 2006, ISSN: 02679477. DOI: 10.1039/b511367a.

[45] M. Kilic, "Validation and measurement uncertainty of the determination of 24 elements in drinking water using ICP-MS," *Water Practice & Technology*, vol. 18, no. 12, pp. 3299–3314, Dec. 2023, ISSN: 1751231X. DOI: 10.2166/wpt.2023.218.

[46] R. S. Pappas, "Sample Preparation Problem Solving for Inductively Coupled Plasma-Mass Spectrometry with Liquid Introduction Systems I. Solubility, Chelation, and Memory Effects," Tech. Rep., May 2012, pp. 20–31.

[47] B. Mei, W. Fong, S. Siu, J. Sai, K. Tee, and S. Tam, "Determination of Mercury in Whole Blood and Urine by Inductively Coupled Plasma Mass Spectrometry," Tech. Rep., 2007. [Online]. Available: https://academic.oup.com/jat/article/31/5/281/775618.

[48] C. F. Harrington, S. A. Merson, and T. M. D' Silva, "Method to reduce the memory effect of mercury in the analysis of fish tissue using inductively coupled plasma mass spectrometry," *Analytica Chimica Acta*, vol. 505, no. 2, pp. 247–254, Mar. 2004, ISSN: 00032670. DOI: 10.1016/j.aca.2003.10.046.

A

Additional ICP-MS data

In this appendix, additional ICP-MS data from experiments not presented in the main part of the thesis are included in the interest of completion.

A.1 Additional tests on foam SS1

Note that the second regeneration and third formation of this foam are missing due to the experiments failing.

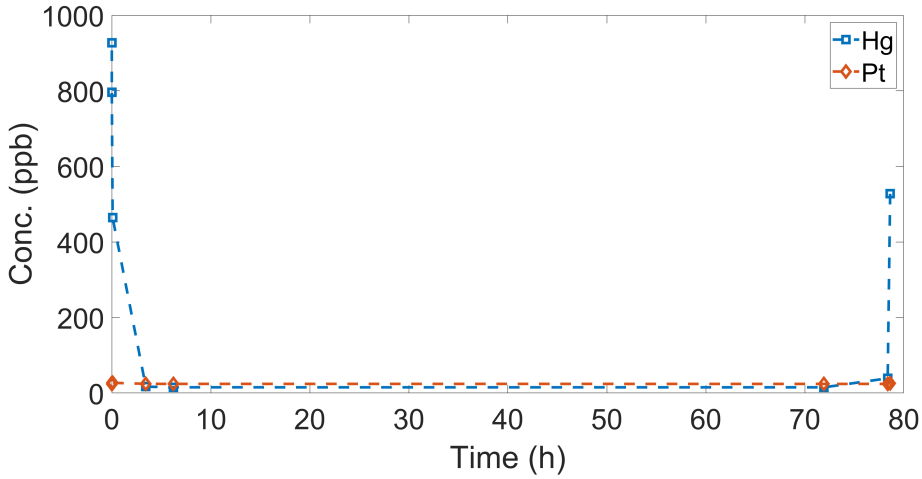

Figure A.1: ICP-MS data from the first formation of foam SS1. Note that the formation potential is turned on right after the first measurement and turned off directly after the second to last measurement.

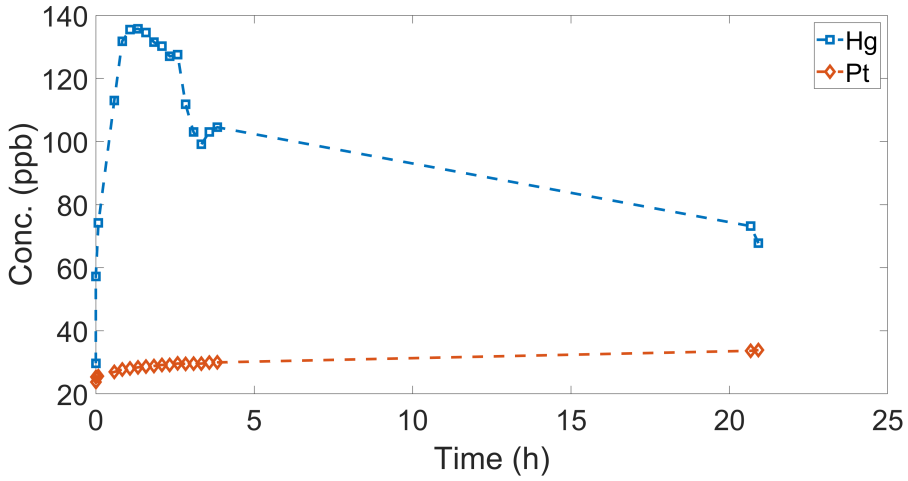

Figure A.2: ICP-MS data from the first regeneration of foam SS1. Note that the regeneration current is turned on right after the first measurement and turned off directly after the second to last measurement.

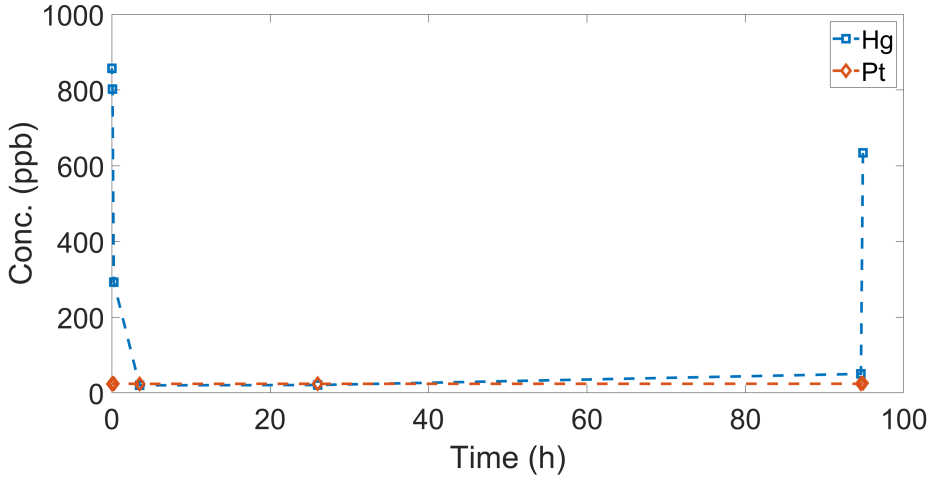

Figure A.3: ICP-MS data from the second formation of foam SS1. Note that the formation potential is turned on right after the first measurement and turned off directly after the second to last measurement.

A.2 Additional tests on foam SS2

Note that the second regeneration and third formation of this foam are missing due to the experiments failing.

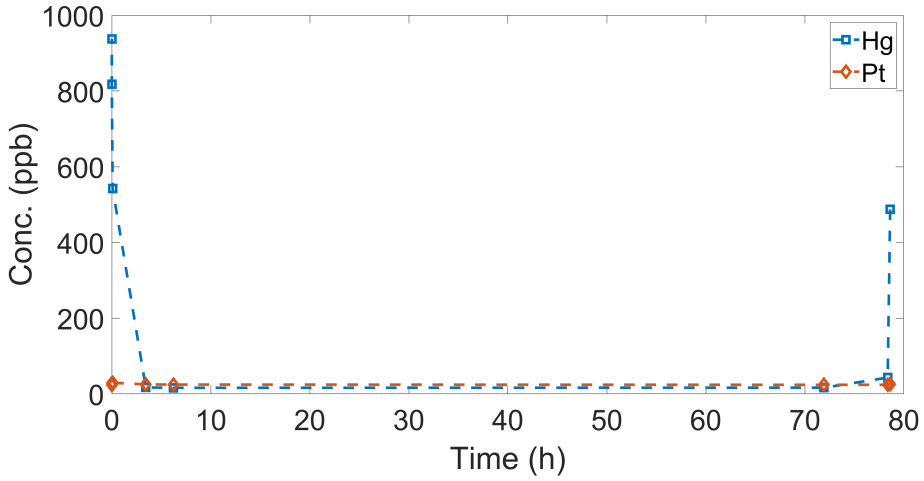

Figure A.4: ICP-MS data from the first formation of foam SS2. Note that the formation potential is turned on right after the first measurement and turned off directly after the second to last measurement.

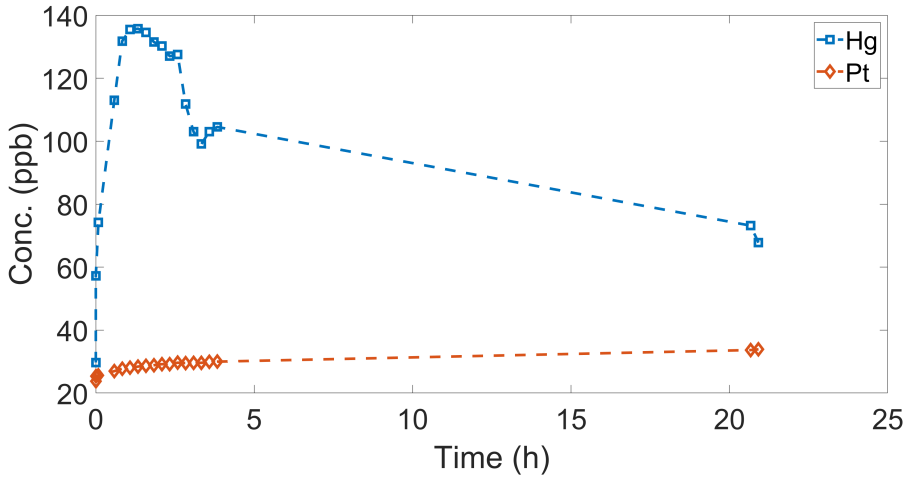

Figure A.5: ICP-MS data from the first regeneration of foam SS2. Note that the regeneration current is turned on right after the first measurement and turned off directly after the second to last measurement.

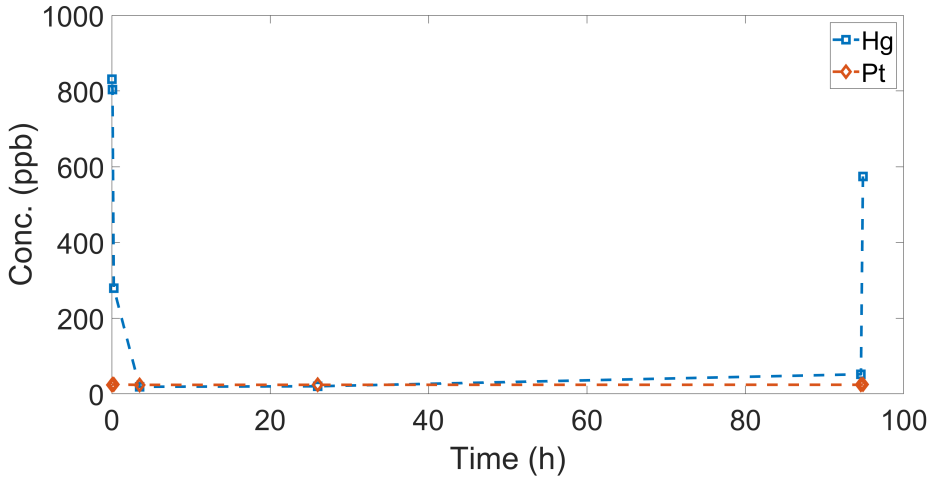

Figure A.6: ICP-MS data from the second formation of foam SS2. Note that the formation potential is turned on right after the first measurement and turned off directly after the second to last measurement.

A.3 Tests on foam SS3

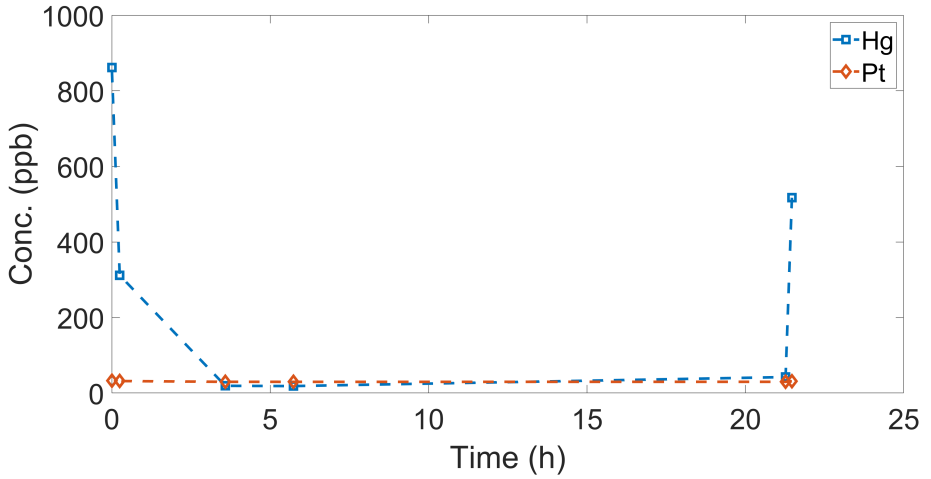

Figure A.7: ICP-MS data from the first formation of foam SS3. Note that the formation potential is turned on right after the first measurement and turned off directly after the second to last measurement.

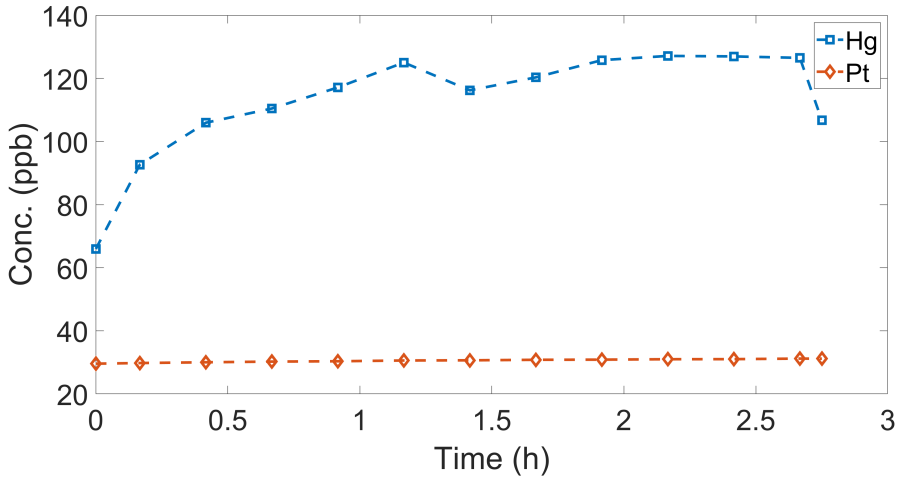

Figure A.8: ICP-MS data from the first regeneration of foam SS3. Note that the regeneration current is turned on right after the first measurement and turned off directly after the second to last measurement.

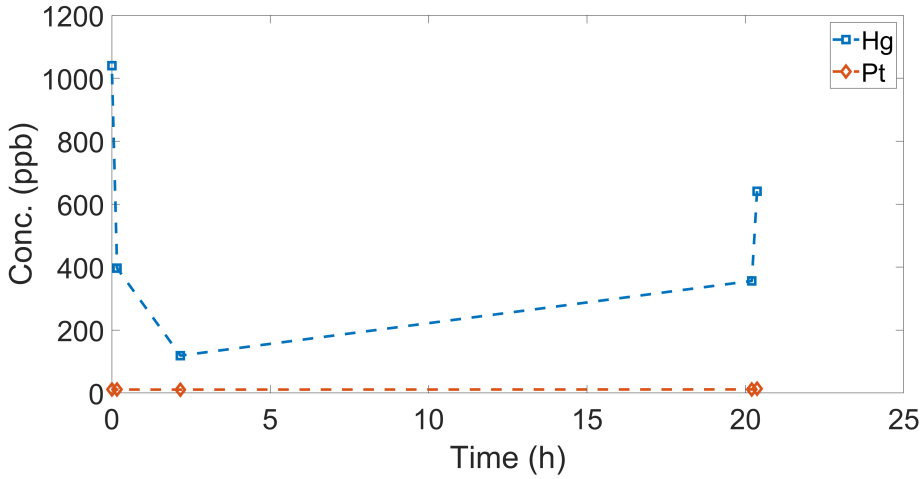

Figure A.9: ICP-MS data from the second formation of foam SS3. Note that the formation potential is turned on right after the first measurement and turned off directly after the second to last measurement.

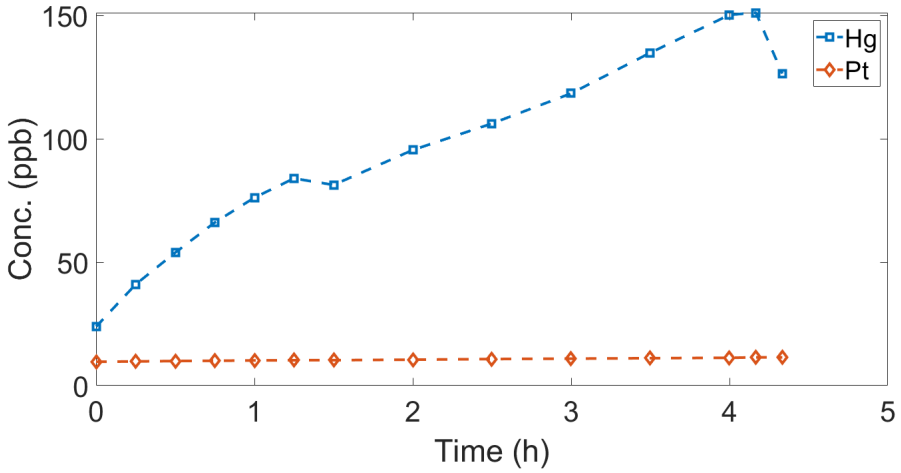

Figure A.10: ICP-MS data from the second regeneration of foam SS3. Note that the regeneration current is turned on right after the first measurement and turned off directly after the second to last measurement.

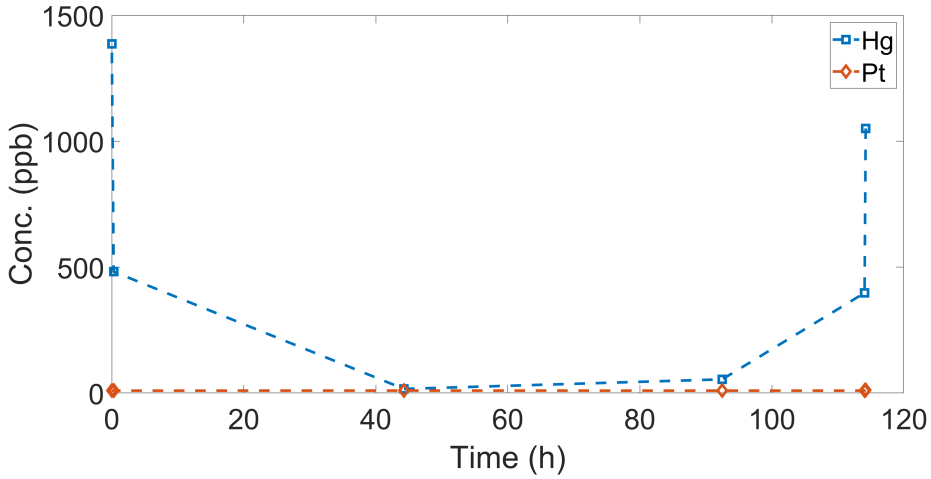

Figure A.11: ICP-MS data from the third formation of foam SS3. Note that the formation potential is turned on right after the first measurement and turned off directly after the second to last measurement.

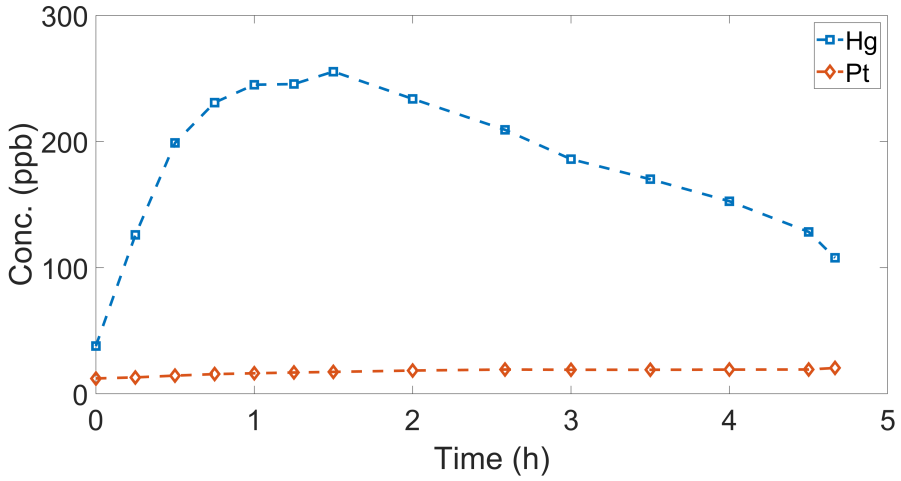

Figure A.12: ICP-MS data from the third regeneration of foam SS3. Note that the regeneration current is turned on right after the first measurement and turned off directly after the second to last measurement.

A.4 Additional RVC foam tests

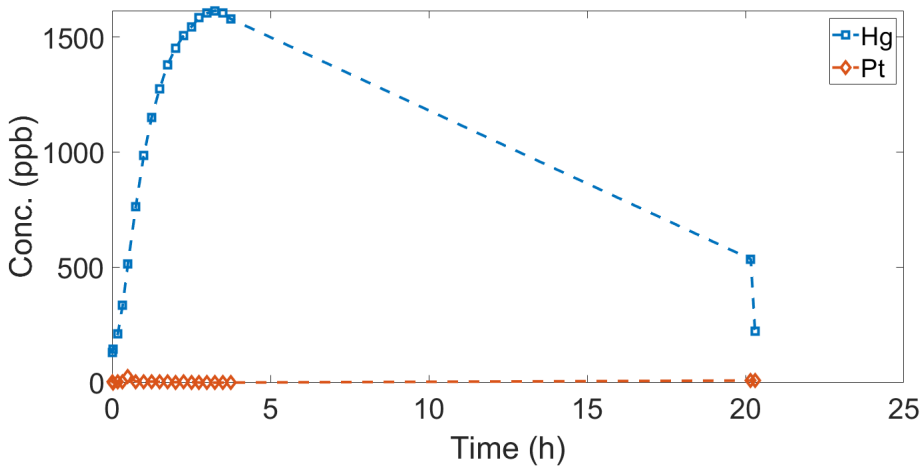

Figure A.13: ICP-MS data from the first regeneration of foam RVC1. Note that the regeneration current is turned on right after the first measurement and turned off directly after the second to last measurement.

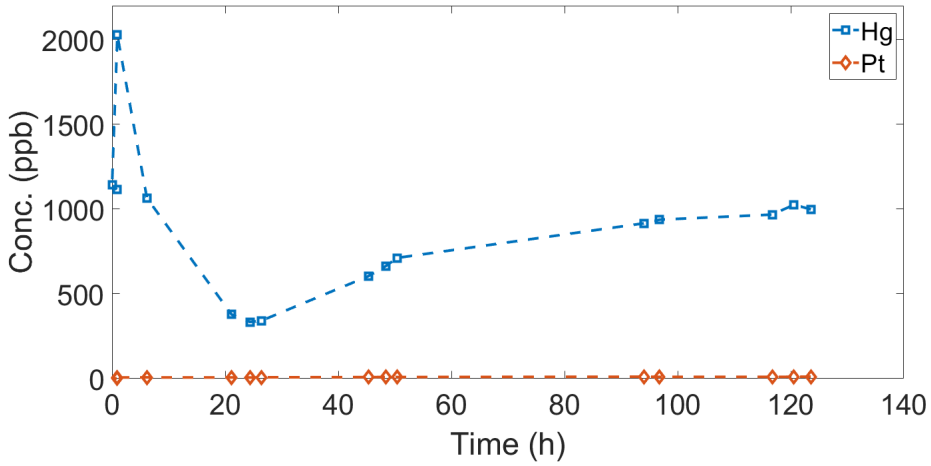

Figure A.14: ICP-MS data from the second formation of foam RVC1. Note that the formation potential is turned on right after the first measurement and turned off directly after the second to last measurement.

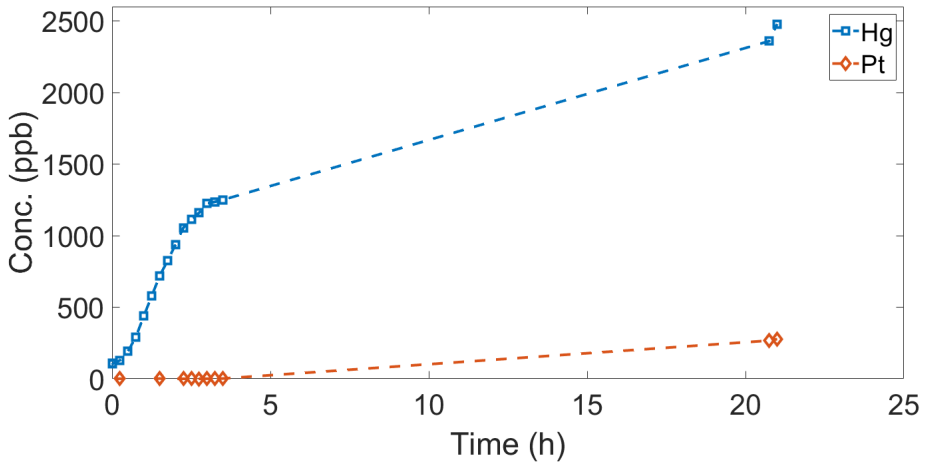

Figure A.15: ICP-MS data from the second regeneration of foam RVC1. Note that the regeneration current is turned on right after the first measurement and turned off directly after the second to last measurement.

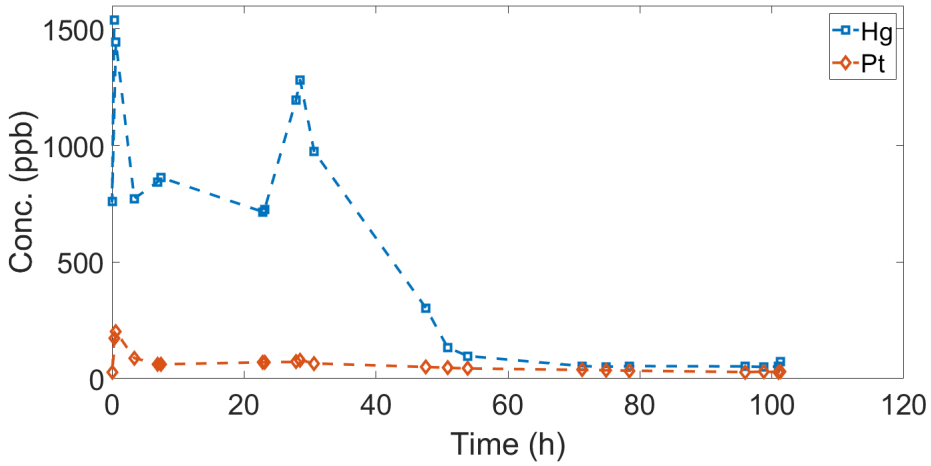

Figure A.16: ICP-MS data from the third formation of foam RVC1. Note that the formation potential is turned on right after the first measurement and turned off directly after the second to last measurement.

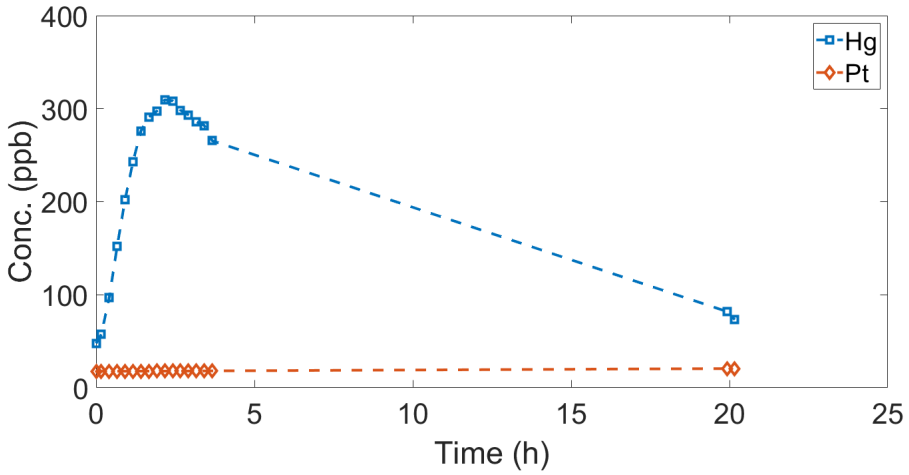

Figure A.17: ICP-MS data from the third regeneration of foam RVC1. Note that the regeneration current is turned on right after the first measurement and turned off directly after the second to last measurement.

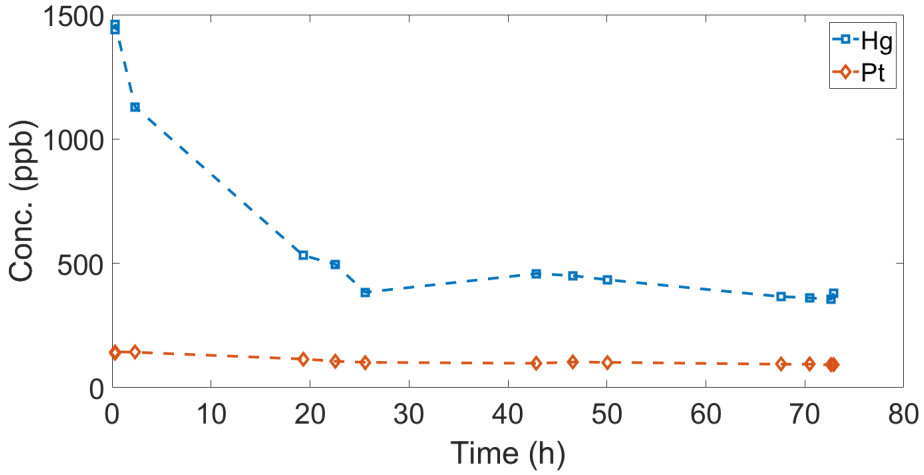

Figure A.18: ICP-MS data from the second formation of foam RVC2. Note that the formation potential is turned on right after the first measurement and turned off directly after the second to last measurement.

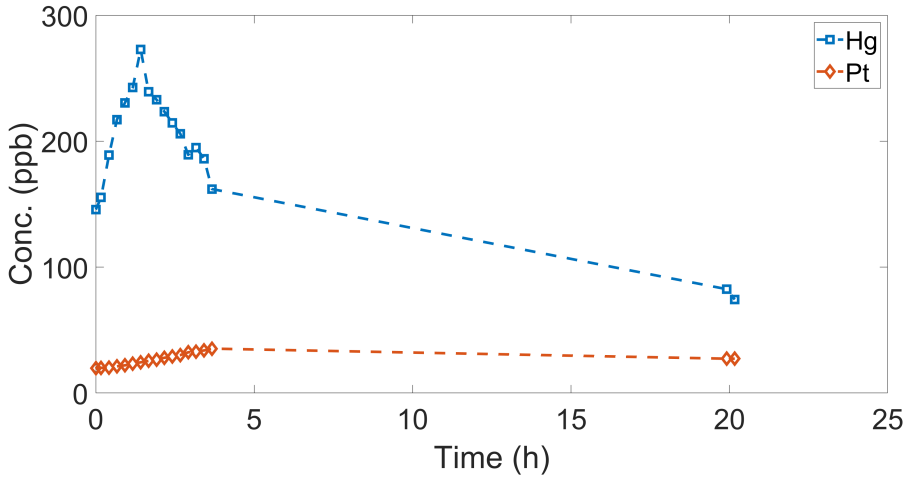

Figure A.19: ICP-MS data from the second regeneration of foam RVC2. Note that the regeneration current is turned on right after the first measurement and turned off directly after the second to last measurement.

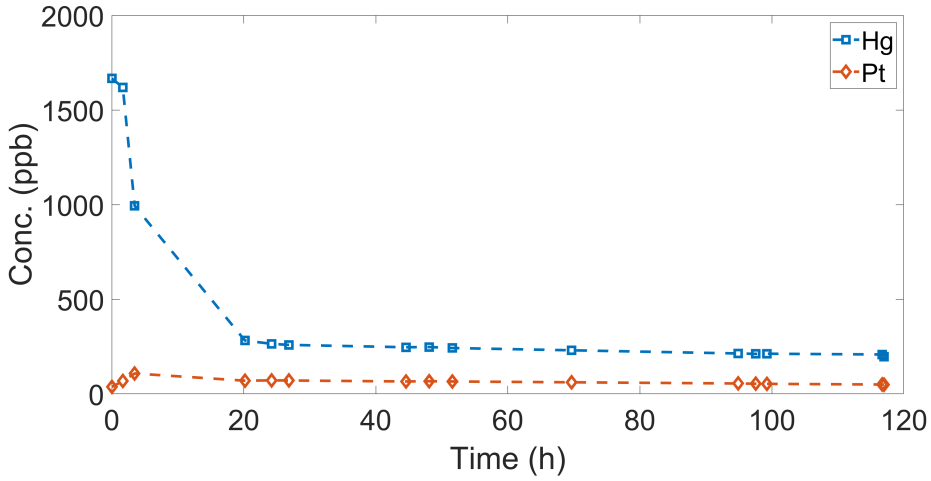

Figure A.20: ICP-MS data from the first formation of foam RVC3. Note that the formation potential is turned on right after the first measurement and turned off directly after the second to last measurement.

B

Schematics of a foam holder

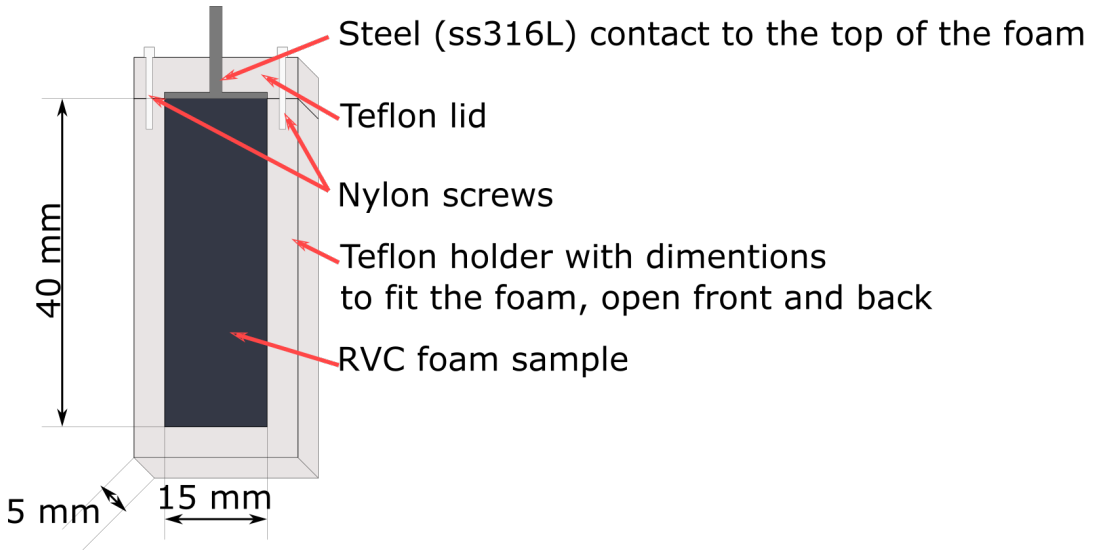

Figure B.1: Schematic of a holder designed to give better electrical contact to foam electrodes. Note that the design was never produced during the thesis work.

DEPARTMENT OF PHYSICS
CHALMERS UNIVERSITY OF TECHNOLOGY
Gothenburg, Sweden
www.chalmers.se

CHALMERS
UNIVERSITY OF TECHNOLOGY